bioRxiv preprint doi: https://doi.org/10.1101/150854; this version posted June 16, 2017. The copyright holder for this preprint (which was not certified by peer review) is the author/funder, who has granted bioRxiv a license to display the preprint in perpetuity. It is made available under aCC-BY-ND 4.0 International license.

1 Title

2 Mechanisms of transmission ratio distortion at hybrid sterility loci within and between
3 *Mimulus* species

4

5 Authors
6 Rachel E. Kerwin[1], Andrea L. Sweigart[1,*]
7
8 Author affiliations
9 [1] Department of Genetics, University of Georgia, Athens, GA 30602
10 *Corresponding author; email: sweigart@uga.edu; phone: (706)-542-7001

11

bioRxiv preprint doi: https://doi.org/10.1101/150854; this version posted June 16, 2017. The copyright holder for this preprint (which was not certified by peer review) is the author/funder, who has granted bioRxiv a license to display the preprint in perpetuity. It is made available under aCC-BY-ND 4.0 International license.

12 **ABSTRACT**

13

14 Hybrid incompatibilities are a common correlate of genomic divergence and a
15 potentially important contributor to reproductive isolation. However, we do not yet have
16 a detailed understanding of how hybrid incompatibility loci function and evolve within
17 their native species, or why they are dysfunctional in hybrids. Here, we explore these
18 issues for a well-studied, two-locus hybrid incompatibility between *hybrid male sterility*
19 *1* (*hms1*) and *hybrid male sterility 2* (*hms2*) in the closely related yellow monkeyflower
20 species *Mimulus guttatus* and *M. nasutus*. By performing reciprocal backcrosses with
21 introgression lines, we find evidence for gametic expression of the *hms1-hms2*
22 incompatibility. Surprisingly, however, hybrid transmission ratios at *hms1* do not reflect
23 this incompatibility, suggesting additional mechanisms counteract the effects of gametic
24 sterility. Indeed, our backcross experiment shows hybrid transmission bias toward *M.*
25 *guttatus* through both pollen and ovules, an effect that is particularly strong when *hms2* is
26 homozygous for *M. nasutus* alleles. In contrast, we find little evidence for *hms1*
27 transmission bias in crosses within *M. guttatus*, providing no indication of selfish
28 evolution at this locus. Although we do not yet have sufficient genetic resolution to
29 determine if hybrid sterility and transmission ratio distortion map to the same loci, our
30 preliminary fine-mapping uncovers a genetically independent hybrid lethality system
31 involving at least two loci linked to *hms1*. This fine-scale dissection of transmission ratio
32 distortion at *hms1* and *hms2* provides insight into genomic differentiation between
33 closely related *Mimulus* species and reveals multiple mechanisms of hybrid dysfunction.

34

bioRxiv preprint doi: https://doi.org/10.1101/150854; this version posted June 16, 2017. The copyright holder for this preprint (which was not certified by peer review) is the author/funder, who has granted bioRxiv a license to display the preprint in perpetuity. It is made available under aCC-BY-ND 4.0 International license.

35 **INTRODUCTION**

36

37 Hybrid incompatibilities are a common outcome of genomic divergence among
38 closely related species. Across diverse taxa, a number of genes for hybrid inviability and
39 sterility have been identified (see Presgraves 2010; Maheshwari and Barbash 2011;
40 Sweigart and Willis 2012; Ouyang and Zhang 2013), but we still know very little about
41 how such genes function and initially evolve within their native species. One possibility
42 is that the initial mutations are selectively neutral and become fixed by random genetic
43 drift. Alternatively, the mutations might increase in frequency because they benefit the
44 native species for reasons that are incidental to their role in reproductive isolation – by
45 promoting ecological adaptation, for example (Schluter and Conte 2009). Yet another
46 possibility is that hybrid incompatibilities arise through recurrent bouts of intragenomic
47 conflict within species (Frank 1991; Hurst and Pomiankowski 1991). In this last scenario,
48 selfish genetic elements (*e.g*., transposons, meiotic drivers, gamete killers) manipulate
49 host reproduction to bias their own transmission. Because these actions are often
50 detrimental to host fitness, there is then selective pressure for compensatory mutations or
51 suppressors to neutralize the effects of selfish evolution (Burt and Trivers 2006).
52 The idea that intragenomic conflict involving segregation distorters might be a
53 major source of hybrid incompatibilities has resurged in recent years (Johnson 2010;
54 McDermott and Noor 2010; Presgraves 2010; Crespi and Nosil 2013), largely due to
55 influential studies in *Drosophila* that have mapped hybrid segregation distortion and
56 hybrid sterility to the same genomic locations (Tao et al. 2001; Phadnis and Orr 2009b;
57 Zhang et al. 2015). In plants, too, classic and recent crossing studies have revealed
58 "gamete killers" that affect both transmission ratios and fertility; at these loci, one
59 parental allele causes the abortion of gametes carrying the other allele (*e.g*., tobacco:
60 (Cameron and Moav 1957), wheat: (Loegering and Sears 1963), tomato: (Rick 1966),
61 rice: (Sano 1990; Long et al. 2008; Yang et al. 2012), Arabidopsis: (Simon et al. 2016)).
62 Although suggestive of a causal link between selfish genetic elements and hybrid
63 incompatibilities, few studies have proven a history of segregation distortion *within*
64 species. Thus, in most cases, an alternative possibility is that segregation distortion acts

bioRxiv preprint doi: https://doi.org/10.1101/150854; this version posted June 16, 2017. The copyright holder for this preprint (which was not certified by peer review) is the author/funder, who has granted bioRxiv a license to display the preprint in perpetuity. It is made available under aCC-BY-ND 4.0 International license.

65 exclusively in hybrid genetic backgrounds, and is a consequence rather than a cause of
66 the incompatibility.
67 In seed plants, hybrid incompatibilities can act in either the diploid sporophyte or
68 the haploid gametophyte, two stages of the life cycle that are controlled by different sets
69 of genes and subject to distinct evolutionary forces (Walbot and Evans 2003; Gossmann
70 et al. 2014; Gossmann et al. 2016). Unlike in animal systems, which have very little
71 haploid gene expression in sperm or egg cells (Braun et al. 1989; Barreau et al. 2008),
72 thousands of genes are expressed in plant gametophytes (*i.e*., pollen and embryo sacs in
73 angiosperms) (Wuest et al. 2010; Rutley and Twell 2015). As a result, hybrid sterility in
74 plants can be caused by genetic incompatibilities that affect the haploid gametophytes or
75 the diploid sporophytic tissues surrounding the gametes (*e.g*., tapetum for pollen, ovule
76 cells for the embryo sac). Of these two possibilities, the former appears to be much more
77 common among the ~50 hybrid sterility loci that have been identified between subspecies
78 of Asian cultivated rice, *Oryza sativa ssp. japonica* and *O. sativa ssp. indica* (Morishima
79 et al. 1991; Ouyang and Zhang 2013). A large number of gametic incompatibilities have
80 also been shown to contribute to transmission ratio distortion in crosses between
81 populations of *Arabidopsis lyrata* (Leppala et al. 2013). This bias toward gametic
82 incompatibilities might be due to differences in the number of mutations that affect the
83 two classes of hybrid sterility and/or to the fact that recessive alleles are exposed in the
84 haploid gametophyte (similar to genes on heteromorphic sex chromosomes).
85 Additionally, rates of evolution might be accelerated for gametophytic genes due to sex-
86 specific selection (Gossmann et al. 2014). It is also possible that intragenomic conflict is
87 more common in the gametophyte; any selfish genetic element that can disable gametes
88 carrying the alternative allele will have a direct impact on its own transmission.
89 Of the handful of plant hybrid sterility genes that have been cloned, all are in rice,
90 most are gametic, and many appear to have evolved via neutral processes. The two most
91 straightforward examples involve pollen defects caused by loss-of-function alleles at
92 duplicate genes (Mizuta et al. 2010; Yamagata et al. 2010), consistent with a model of
93 divergent resolution via degenerative mutations and genetic drift (Werth and Windham
94 1991; Lynch and Force 2000). The remaining six cases all involve gamete killers (Long
95 et al. 2008; Kubo et al. 2011; Yang et al. 2012; Kubo et al. 2016a; Kubo et al. 2016b; Yu

bioRxiv preprint doi: https://doi.org/10.1101/150854; this version posted June 16, 2017. The copyright holder for this preprint (which was not certified by peer review) is the author/funder, who has granted bioRxiv a license to display the preprint in perpetuity. It is made available under aCC-BY-ND 4.0 International license.

96 et al. 2016), which might be taken as evidence for pervasive selfish evolution within rice
97 species. However, molecular characterization of these hybrid sterility systems has
98 provided little support for this scenario. For example, the *S5* locus causes female sterility
99 in *japonica*-*indica* hybrids when gametes carry an incompatible combination of "killer"
100 and "protector" alleles at three, tightly linked genes (Yang et al. 2012). The two
101 domesticated subspecies carry null alleles in distinct components of the killer-protector
102 system. Because both derived haplotypes are perfectly compatible with the ancestral
103 haplotype, it seems unlikely that they entailed fitness costs. Although it is conceivable
104 that intragenomic conflict played a role in the initial formation of the *S5* haplotype (*i.e.*,
105 the ancestral killer/protector combination might represent a resolved conflict), it does not
106 seem to be the cause of the current reproductive barrier between *japonica* and *indica*.
107 Similarly, at the *Sa* locus, which causes *japonica*-*indica* hybrid male sterility, patterns of
108 molecular variation and the prevalence of "neutral" alleles that are compatible in all
109 crosses suggest that hybrid dysfunction may have evolved unopposed by natural selection
110 (Long et al. 2008; Sweigart and Willis 2012). A key feature of these gamete killers is that
111 they are caused by two or more tightly linked, epistatic genes (Long et al. 2008; Yang et
112 al. 2012; Kubo 2013; Kubo et al. 2016a). Adding to the complexity, some of them require
113 additional, unlinked loci that act sporophytically (Kubo et al. 2011; Kubo et al. 2016a;
114 Kubo et al. 2016b). Taken together, these studies suggest that hybrid sterility in rice is
115 polygenic and might evolve without significant fitness costs within species. However, it
116 is not yet clear if these themes are generalizable to other plant systems.

117 Here we investigate patterns of transmission ratio distortion associated with a
118 two-locus hybrid sterility system between the closely related monkeyflower species,
119 *Mimulus guttatus* and *M. nasutus*. Previously, we fine-mapped the two incompatibility
120 loci – *hybrid male sterility 1* (*hms1*) and *hybrid male sterility 2* (*hms2*) – to small nuclear
121 genomic regions of ~60 kb each on chromosomes 6 and 13 (Sweigart and Flagel 2015).
122 We also discovered evidence that the *hms1* incompatibility allele is involved in a partial
123 selective sweep within a single population of *M. guttatus*, but the underlying cause of the
124 sweep is unknown (Sweigart and Flagel 2015). Additionally, because the *hms1* sterility
125 allele is embedded in a nearly invariant, 320-kb haplotype, it is not yet clear whether
126 *hms1* or a linked locus is the target of the sweep. This polymorphic hybrid sterility

bioRxiv preprint doi: https://doi.org/10.1101/150854; this version posted June 16, 2017. The copyright holder for this preprint (which was not certified by peer review) is the author/funder, who has granted bioRxiv a license to display the preprint in perpetuity. It is made available under aCC-BY-ND 4.0 International license.

127 system provides a unique opportunity to test directly whether selfish evolution within
128 species can lead to incompatibilities between species.

129 Previously, in crosses between *M. guttatus* and *M. nasutus*, we observed
130 transmission ratio distortion (TRD) of genotypes at both *hms1* and *hms2* (Sweigart et al.
131 2006; Sweigart and Flagel 2015), but the causes have remained unexplored. Additionally,
132 these previous studies did not test directly whether the *hms1-hms2* incompatibility acts in
133 the gametophyte or sporophyte, although patterns of F_2 hybrid sterility seemed to suggest
134 the latter. Results from these studies suggested that the incompatibility acts in the diploid
135 sporophyte with the *M. guttatus* allele at *hms1* acting dominantly in combination with
136 recessive *M. nasutus* alleles at *hms2* to cause nearly complete male sterility and partial
137 female sterility (Sweigart et al. 2006). Consistent with this genetic model, pollen viability
138 is ~20% in F_2 hybrids that are heterozygous for *hms1* and homozygous for *M. nasutus*
139 alleles at *hms2* ($hms1_{GN}$; $hms2_{NN}$), much lower than the 50% expected for a strictly
140 gametic hybrid incompatibility (with $hms1_{G}$; $hms2_{N}$ causing dysfunction). Moreover,
141 because a gametic hybrid incompatibility should cause transmission bias at *both*
142 interacting loci, we would expect a deficit of *M. guttatus* alleles at *hms1* equal to that of
143 *M. nasutus* alleles at *hms2*. Although F_2 hybrids do indeed show a deficit of *M. nasutus*
144 alleles at *hms2*, allelic transmission at *hms1* follows the Mendelian expectation (Sweigart
145 et al. 2006).

146 In the current study, we used introgression lines (ILs) and a reciprocal backcross
147 design to distinguish among at least four possibilities for TRD in genomic regions linked
148 to *hms1* and *hms2:* 1) distortion through male gametes due to pollen competition and/or
149 pollen sterility, 2) distortion through female gametes due to female meiotic drive (*e.g.*,
150 (Fishman and Saunders 2008) and/or ovule sterility, 3) TRD through both male and
151 female gametes due to an incompatibility that affects both gametophytes (*e.g.*, (Kubo et
152 al. 2016a), and 4) distortion caused by selection against zygotes. In a series of crossing
153 experiments, we investigated the mechanism of TRD at *hms1* and *hms2* and addressed the
154 following specific questions. Is hybrid transmission bias at *hms1* and/or *hms2* a simple
155 byproduct of gametic hybrid sterility? Is there evidence for hybrid transmission bias at
156 these loci independent of gamete sterility? Are hybrid sterility and TRD genetically
157 separable? Does TRD at *hms1* occur within *M. guttatus*? Our results provide insight into

bioRxiv preprint doi: https://doi.org/10.1101/150854; this version posted June 16, 2017. The copyright holder for this preprint (which was not certified by peer review) is the author/funder, who has granted bioRxiv a license to display the preprint in perpetuity. It is made available under aCC-BY-ND 4.0 International license.

158 the mechanisms of hybrid sterility and transmission distortion, and into the evolutionary
159 dynamics of incompatibility alleles within species.
160
161
162 **METHODS**
163
164 **Study system and plant lines**
165 The *Mimulus guttatus* species complex is a group of phenotypically diverse wildflowers
166 with abundant natural populations throughout much of western North America. In this
167 study, we focus on *M. guttatus* and *M. nasutus*, two members of the complex that
168 diverged roughly 200,000 years ago (Brandvain et al. 2014). These species occupy a
169 partially overlapping range, and are primarily differentiated by mating system. *M.*
170 *guttatus* is predominantly outcrossing with showy, insect-pollinated flowers, whereas *M.*
171 *nasutus* is highly self-fertilizing with reduced flowers. In geographic regions where the
172 two species co-occur, they are partially reproductively isolated by differences in floral
173 morphology, flowering phenology, and pollen-pistil interactions (Diaz and Macnair 1999;
174 Martin and Willis 2007; Fishman et al. 2014). Hybrid incompatibilities are also common,
175 but variable (Vickery 1978; Christie and Macnair 1987; Sweigart et al. 2007; Case and
176 Willis 2008; Martin and Willis 2010). Despite these barriers to interspecific gene flow,
177 sympatric populations display evidence of genome-wide introgression (Sweigart and
178 Willis 2003; Brandvain et al. 2014; Kenney and Sweigart 2016).
179 Previous work identified two nuclear incompatibility loci – *hybrid male sterility 1*
180 (*hms1*) and *hybrid male sterility 2* (*hms2*) – that cause nearly complete male sterility and
181 partial female sterility in a fraction of F_2 hybrids between an inbred line of *M. guttatus*
182 from Iron Mountain, Oregon (IM62), and a naturally inbred *M. nasutus* line from
183 Sherar's Falls, Oregon (SF5) (Sweigart et al. 2006). In 2015, Sweigart and Flagel
184 generated a large SF5-IM62 F_2 mapping population (N = 5487) to fine map *hms1* and
185 *hms2* to regions of ~60 kb on chromosome 6 and chromosome 13, respectively. Hybrids
186 carrying at least one incompatible *M. guttatus* allele at *hms1* in combination with two
187 incompatible *M. nasutus* alleles at *hms2* display extreme male sterility and partial female
188 sterility (Sweigart et al. 2006). Furthermore, the *hms1* locus is polymorphic within the

bioRxiv preprint doi: https://doi.org/10.1101/150854; this version posted June 16, 2017. The copyright holder for this preprint (which was not certified by peer review) is the author/funder, who has granted bioRxiv a license to display the preprint in perpetuity. It is made available under aCC-BY-ND 4.0 International license.

189 Iron Mountain population (Sweigart et al. 2007) and several inbred lines derived from
190 that site are known to carry "compatible" alleles that do not cause hybrid sterility when
191 crossed to *M. nasutus* (Sweigart and Flagel 2015). In experimental crosses to test for
192 TRD at *hms1* within *M. guttatus*, we used a compatible line called IM767. In total, three
193 inbred lines were used in different crossing schemes to test for TRD within and between
194 species (see below). SF5 is compatible at *hms1* and incompatible at *hms2,* IM62 is
195 incompatible at *hms1* and compatible at *hms2*, and IM767 is compatible at *hms1* and
196 *hms2*.
197 All plants were grown in the greenhouse at the University of Georgia. For all
198 crosses, seeds were planted into 96-cell flats containing Fafard 3B potting mix (Sun Gro
199 Horticulture, Agawam, MA), stratified for 7 days at 4°C, and then placed in a greenhouse
200 with supplemental lights set to 16-hr days. Plants were bottom-watered daily and
201 temperatures were maintained at 24°C during the day and 16°C at night.
202
203 **Introgression line (IL) crossing design to investigate mechanisms of transmission**
204 **ratio distortion between *M. guttatus* and *M. nasutus***
205 Previously, two reciprocal nearly isogenic line (NIL) populations carrying *M. nasutus*
206 (SF5) or *M. guttatus* (IM62) introgressions in the opposite genetic background were
207 generated (Fishman and Willis 2005). Briefly, a single SF5 x IM62 F_1 and IM62 x SF5 F_1
208 individual each served as the initial seed parent then underwent four generations of
209 backcrossing to create a BN_4 NIL population (SF5 x IM62 F_1, *M. nasutus* recurrent
210 parent) and BG_4 NIL population (IM62 x SF5 F_1, *M. guttatus* recurrent parent). Within
211 the BN_4 and BG_4 populations, each NIL carries a unique complement of heterozygous
212 introgressions in a genome that is expected to be 96.875% homozygous for the recurrent
213 parent's alleles. To determine the genomic locations of the heterozygous introgressed
214 regions, the NILs were genotyped at microsatellite and gene-based markers distributed
215 throughout the genome (L. Fishman, unpublished). We selected three NILs with
216 introgressions spanning *hms1* or *hms2* for further genetic analyses. Against a largely *M.*
217 *guttatus* background, the BG_4.476 NIL is heterozygous for an introgression that includes
218 *hms1* and ~78% of the physical distance along chromosome 6. The BG_4.149 line is
219 heterozygous for an introgression that spans ~71% of chromosome 13 and includes *hms2*.

bioRxiv preprint doi: https://doi.org/10.1101/150854; this version posted June 16, 2017. The copyright holder for this preprint (which was not certified by peer review) is the author/funder, who has granted bioRxiv a license to display the preprint in perpetuity. It is made available under aCC-BY-ND 4.0 International license.

220 Against a *M. nasutus* background, the BN_4.62 line is heterozygous for ~75% of
221 chromosome 13, including *hms2*. In addition to these NILs, we used an *hms1*
222 introgression line, RSB_4, created after four generations of recurrent selection for hybrid
223 sterility with backcrossing to *M. nasutus,* starting from a sterile SF5-IM62 BC_1 individual
224 (Sweigart et al. 2006); the heterozygous introgression spans ~50% of chromosome 6.

225 To characterize TRD between *M. guttatus* and *M. nasutus*, we used a multi-step
226 crossing scheme, starting with the NILs and RSB_4 (described above), to create a set of
227 lines carrying specific two-locus genotypes at *hms1* and *hms2*. First, to generate
228 introgression lines (ILs) that carry heterozygous alleles at both *hms1* and *hms2* in an
229 otherwise *M. guttatus* or *M. nasutus* genetic background, we crossed BG_4.476 to
230 BG_4.149, and BN_4.62 to RSB_4. From those progeny, we identified *hms1-hms2* double
231 heterozygotes by genotyping markers that flank *hms1* (M8 and M24) and *hms2* (M51 and
232 MgSTS193), as described previously (Sweigart and Flagel 2015). Next, to generate
233 individuals that carry various two-locus combinations at *hms1* and *hms2*, we self-
234 fertilized doubly heterozygous ILs from each genetic background (*i.e.*, IL-G and IL-N =
235 *M. guttatus* and *M. nasutus* backgrounds, respectively). These crosses are expected to
236 yield nine different two-locus genotypes each (typical of an F_2), five of which are
237 heterozygous at *hms1* and/or *hms2* (Figure 1). Surprisingly, one of the relevant IL-N
238 *hms1-hms2* genotypes was not recovered (*hms1*$_{GG}$; *hms2*$_{GN}$, see Figure 1); the *hms1*-
239 introgression could not be made homozygous for *M. guttatus* alleles against an *M.*
240 *nasutus* genetic background (see Results). We assessed male fertility (*i.e.*, pollen
241 viability) for the nine experimental IL genotypes (five for IL-G and four for IL-N) as
242 described previously (Sweigart et al. 2006; Sweigart et al. 2007).

243 To test the effect of *hms1* genotype on transmission at *hms2* and vice versa, we
244 reciprocally backcrossed each of the nine ILs to both *M. guttatus* (IM62) and *M. nasutus*
245 (SF5) (Figure 1). Thus, for each IL, we generated four reciprocal backcross populations
246 allowing us to dissect gender-specific transmission ratio distortion. For each IL, two of
247 the backcrosses used the emasculated IL as the seed parent in crosses to IM62 and SF5
248 lines (i.e., IL-IM62 and IL-SF5) and two used the IL as the pollen parent in crosses to
249 emasculated IM62 and SF5 plants (i.e., IM62-IL, and SF-IL). If *hms* distortion occurs
250 through pollen (due to pollen competition or a gametic incompatibility), we expect TRD

bioRxiv preprint doi: https://doi.org/10.1101/150854; this version posted June 16, 2017. The copyright holder for this preprint (which was not certified by peer review) is the author/funder, who has granted bioRxiv a license to display the preprint in perpetuity. It is made available under aCC-BY-ND 4.0 International license.

251 in one or both of the backcrosses using the IL as the paternal parent, but not as the
252 maternal parent. If, instead, female meiotic drive and/or a female gametic incompatibility
253 occurs at these *hms* loci, we would expect to see TRD in both backcrosses with the IL as
254 the seed parent, but not with the IL as the pollen parent. Finally, if TRD is caused by the
255 loss of diploid zygotes (or seedlings), it should be apparent in *both* reciprocal crosses to
256 the same recurrent parent (*i.e.*, regardless of the gender of the IL). For all crosses, the
257 female parent was emasculated 1-2 days before hand-pollination to prevent self-
258 pollination. Sample sizes for the progeny classes ranged from 33 to 215 individuals
259 (average $N = 136$).
260 For each *hms* locus, we performed factorial ANOVAs in Jmp Pro 13.0 to examine
261 if genotype ratios were affected by four factors: 1) IL genetic background, 2) IL genotype
262 at the interacting *hms* locus, 3) backcross direction, and 4) identity of the recurrent
263 parent.
264
265 **Crossing design to examine transmission ratio distortion within *M. guttatus***
266 To determine whether transmission ratio distortion at the polymorphic *hms1*
267 incompatibility locus occurs between incompatible and compatible alleles from the Iron
268 Mountain population of *M. guttatus*, we generated reciprocal F_2 and backcrossed
269 populations with IM62 and IM767. We previously determined that the IM767 inbred line
270 carries a compatible allele at *hms1* (*i.e.*, one that does not carry the 320-kb haplotype or
271 cause sterility in combination with SF5 alleles at *hms2*). The IM62 and IM767 inbred
272 lines were intercrossed reciprocally and a single F_1 hybrid from each was self-fertilized to
273 form reciprocal F_2 populations (IM62 x IM767: $N = 267$; IM767 x IM62: $N = 315$). To
274 identify putative female- and male-specific sources of TRD, and to distinguish between
275 meiotic/gametic mechanisms versus zygotic selection, we generated reciprocal
276 backcrosses with IM62 and IM767. We used a single F_1 hybrid (IM62 x 767; maternal
277 parent listed first) to generate four backcross populations to the recurrent parents (F_1-
278 IM62 BC_1, IM62-F_1 BC_1, F_1-IM767 BC_1, IM767-F_1 BC_1). Two of these backcrosses used
279 the emasculated F_1 as the seed parent and two used the F_1 as the pollen donor in crosses
280 to the emasculated recurrent parents.

bioRxiv preprint doi: https://doi.org/10.1101/150854; this version posted June 16, 2017. The copyright holder for this preprint (which was not certified by peer review) is the author/funder, who has granted bioRxiv a license to display the preprint in perpetuity. It is made available under aCC-BY-ND 4.0 International license.

281 We also wanted to examine the effect of *M. nasutus hms2* alleles on patterns of
282 within-*M. guttatus* TRD at *hms1*. We wondered if having *M. nasutus* alleles at *hms2* has
283 the potential to unleash severe distortion at *hms1*, even in an otherwise *M. guttatus*
284 genetic background. To address this question, we intercrossed IM767 with a BG_4-NIL
285 (BG_4.275) that is heterozygous for an SF5 introgression spanning ~36% of chromosome
286 13 including *hms2* (in an IM62 genetic background; Figure S2). We self-fertilized two of
287 the resulting F_1s to generate F_2 hybrids segregating for SF5 alleles at *hms2* against an
288 IM62-IM767 F_2-like genetic background. We then genotyped at *hms*-linked markers
289 (M183 for *hms1* and MgSTS193 for *hms2*) to identify IM62-IM767 *hms1* heterozygotes
290 in combination with three different *hms2* genotypes: 1) IM62 homozygotes, 2) IM767
291 homozygotes, or 3) SF5 homozygotes. Using each of these three genotypic classes, we
292 performed reciprocal backcrosses to IM767 (Figure S2).
293
294 **Assessment of transmission ratio distortion**
295 To examine patterns of TRD at the *hms1* and *hms2* loci, we collected leaf tissue from
296 individual plants and isolated genomic DNA using a rapid extraction protocol (Cheung *et*
297 *al*. 1993) modified for 96-well format. To infer the *hms1* and *hms2* genotypes of hybrid
298 progeny generated from crosses between IM62 and SF5, we determined genotypes at a
299 multiplexed set of fluorescently labeled markers that flank *hms1* (M8 and M24) and *hms2*
300 (MgSTS193 and M51) following amplification protocols used previously (Sweigart et al.
301 2006; Sweigart et al. 2007). We excluded individuals with crossovers between either pair
302 of flanking markers; based on expected frequency of double crossovers between flanking
303 markers, genotyping error rates for *hms1* and *hms2* were each < 1%. For experimental
304 crosses involving IM62 and IM767, only one tightly linked marker was used to infer
305 genotype at *hms1* (M183). Based on expected crossovers between *hms1* and M183, the
306 genotyping error rate was < 1%. All fluorescently labeled marker products were run on
307 an ABI 3730 at the University of Georgia Genomics Facility. Genotypes were scored
308 automatically using GeneMarker (SoftGenetics), with additional hand scoring when
309 necessary. We used chi-square tests with two degrees of freedom to determine if *hms*-
310 linked genotypes were significantly distorted.
311

bioRxiv preprint doi: https://doi.org/10.1101/150854; this version posted June 16, 2017. The copyright holder for this preprint (which was not certified by peer review) is the author/funder, who has granted bioRxiv a license to display the preprint in perpetuity. It is made available under aCC-BY-ND 4.0 International license.

312 **RESULTS**

313

314 **Transmission ratio distortion in *M. nasutus-M. guttatus* F_2 hybrids**

315 As part of previous efforts to fine-map *Mimulus* hybrid incompatibility loci (Sweigart and
316 Flagel 2015), we generated a large *M. nasutus-M. guttatus* F_2 hybrid mapping population
317 (N = 5487) and genotyped all individuals at gene-based markers flanking *hms1* (M8 and
318 M24) and *hms2* (M51 and MgSTS193). As previously reported (Sweigart et al. 2006;
319 Sweigart and Flagel 2015), we observed significant transmission ratio distortion (TRD) in
320 F_2 genotypes at both hybrid sterility loci (Table 1). At *hms1*, we observed a significant
321 excess of heterozygotes, but allelic transmission did not differ from the Mendelian
322 expectation. The observed genotype ratios at *hms1* also differed significantly from the
323 expectation given the random union of two gametes with the observed allele frequencies.
324 At *hms2*, we observed an excess of *M. guttatus* homozygotes and a deficit of *M. nasutus*
325 homozygous genotypes, as well as a significant bias toward *M. guttatus* alleles. However,
326 genotype ratios at *hms2* do not differ from what is expected given the observed allele
327 frequencies. Taken together, these patterns suggest TRD at *hms1* might be driven
328 primarily by zygotic selection, whereas *hms2* appears to be influenced primarily by
329 selection among gametes.

330 When considered together, the two-locus genotypes at *hms1* and *hms2* differ
331 significantly from the Mendelian expectation (X^2 = 389.372, d.f. = 8, P < 0.0001, N =
332 5487). Although the two-locus genotypes are also significantly different from the
333 expectation given the observed allele frequencies at *hms1* and *hms2* shown in Table 1 (X^2
334 = 71.626, d.f. = 8, P <0.0001), the values are much more closely aligned (Table 2).
335 Particularly notable is the deficit of two genotypic classes ($hms1_{GG}$; $hms2_{NN}$ and $hms1_{NN}$;
336 $hms2_{GG}$) and the excess of two others ($hms1_{GG}$; $hms2_{GG}$ and $hms1_{NN}$; $hms2_{NN}$; Table 2).
337 This pattern of two-locus disequilibrium follows the expectation for gametic action of
338 *hms1-2* sterility (*i.e.*, with $hms1_G$; $hms2_N$ gametes tending to be sterile). However, the
339 observed F_2 transmission ratios at *hms1* and *hms2* cannot be entirely explained by $hms1_G$;
340 $hms2_N$ gametic sterility (Table S1). This phenomenon, whether acting through one or
341 both parents, would be expected to reduce the transmission of *M. guttatus* alleles at *hms1*,
342 in the same way that it reduces *M. nasutus* alleles at *hms2*. However, there is no

bioRxiv preprint doi: https://doi.org/10.1101/150854; this version posted June 16, 2017. The copyright holder for this preprint (which was not certified by peer review) is the author/funder, who has granted bioRxiv a license to display the preprint in perpetuity. It is made available under aCC-BY-ND 4.0 International license.

343 indication of allelic transmission bias at *hms1* in the F_2 hybrids. Taken together, these
344 results suggest that gametic expression of the *hms1-hms2* incompatibility is important,
345 but not the sole contributor, to patterns of transmission ratio distortion in F_2 hybrids.
346

347 ***M. nasutus-M. guttatus* IL crosses reveal multiple causes of F_2 distortion**

348 To investigate several possible causes of F_2 transmission ratio distortion at *hms1* and
349 *hms2*, we performed a crossing experiment using the IL-G and IL-Ns. In this crossing
350 design (Figure 1), individuals with one of several possible two-locus *hms1-hms2*
351 genotypes – in each of the IL genetic backgrounds – were crossed reciprocally to *M.*
352 *guttatus* (IM62) and *M. nasutus* (SF5). By scoring *hms1* and *hms2* genotypes in the
353 progeny of these crosses, we were able to examine the effects of several factors,
354 including parental genotype, genetic background, and cross direction, on transmission
355 ratios at the two hybrid sterility loci. Of the 36 crosses performed, 12 showed significant
356 transmission ratio distortion at *hms1* and/or *hms2* (Table 3; note that two crosses were
357 unsuccessful due to hybrid male sterility). For both *hms1* and *hms2*, parental genotype at
358 one locus has a strong effect on allelic transmission at the other (*hms1* affects *hms2*: $F =$
359 37.69, $P < 0.0001$; *hms2* affects *hms1*: $F = 7.80$, $P = 0.004$; Figure S1). For *hms2*, cross
360 direction is also important, with stronger TRD occurring through pollen ($F = 72.33$, $P <$
361 0.0001). Neither the genetic background nor the identity of the recurrent parent
362 significantly affected transmission ratios at *hms1* or *hms2* (results not shown).

363 The pattern of TRD at *hms2* follows what is expected if hybrid sterility acts
364 through gametes. For example, if pollen grains are inviable when they carry *M. guttatus*
365 alleles at *hms1* in combination with *M. nasutus* alleles at *hms2*, the effect of *hms1*
366 paternal genotype on TRD at *hms2* should be additive. Indeed, progeny from males that
367 carry one or two *M. guttatus* alleles at *hms1* show a 28% or 76% under-transmission of
368 *M. nasutus* alleles at *hms2* relative to the Mendelian expectation (Figure S1). Consistent
369 with the action of a gametic incompatibility, backcross progeny of doubly heterozygous
370 IL parents (*i.e.*, $hms1_{GN}$; $hms2_{GN}$) are much less likely to come from gametes with an *M.*
371 *guttatus* allele at *hms1* in combination with an *M. nasutus* allele at *hms2* (Table 4). In
372 these crosses, the $hms1_{G}$; $hms2_{N}$ gamete type is under-transmitted through both sexes,

bioRxiv preprint doi: https://doi.org/10.1101/150854; this version posted June 16, 2017. The copyright holder for this preprint (which was not certified by peer review) is the author/funder, who has granted bioRxiv a license to display the preprint in perpetuity. It is made available under aCC-BY-ND 4.0 International license.

373 though the effect is stronger through males. Under-transmission is also more severe in
374 crosses to IM62 (*M. guttatus*) and against the IL-N genetic background (Table S2).

375 If the *hms1-hms2* incompatibility acts through gametes, we might expect patterns
376 of pollen viability to predict rates of transmission ratio distortion through males. To
377 examine this possibility, we measured pollen viability in various two-locus genotypes of
378 the IL-G and IL-Ns (Table 5). In general, patterns of male fertility and transmission ratio
379 distortion are indeed related. For example, pollen viability is 64% in IL-Gs that are
380 $hms1_{GG}$; $hms2_{GN}$. For this genotype, if we assume equal transmission of *M. guttatus* and
381 *M. nasutus* alleles into pollen and attribute all sterility to $hms1_{G}$; $hms2_{N}$, then the *M.*
382 *guttatus* allele at *hms2* should be present in 78% of progeny when this individual is used
383 as the paternal parent in a cross (which is close to the observed frequency of 86%, Table
384 3). Similarly, for IL-Gs that are $hms1_{GN}$; $hms2_{GN}$, if we assume that all $hms1_{G}$; $hms2_{N}$
385 gametes are inviable (and divide the remaining 7% sterility equally among the other three
386 two-locus genotypes), we expect *M. guttatus* allele frequencies of 33% and 66% at *hms1*
387 and *hms2*, respectively. These values are very similar to what we observe when this IL-G
388 genotype is backcrossed to *M. guttatus* (37% and 67%, Table 3).

389 At *hms1*, TRD is more complex. On the one hand, *M. guttatus* alleles at *hms1* are
390 under-transmitted due to the $hms1_{G}$; $hms2_{N}$ gametic sterility discussed above (Table S2).
391 On the other hand, in many of the IL-backcrosses, *M. guttatus* alleles at *hms1* are
392 overrepresented among the progeny (Tables 2 and 2.1). This effect is most pronounced
393 when the IL parent is heterozygous at *hms1* and homozygous for *M. nasutus* alleles at
394 *hms2* (Figure S1; note that this genotype is not completely sterile so crosses can still be
395 performed). Remarkably, this direction of TRD is exactly the opposite of what is
396 expected if *hms1* transmission is primarily influenced by the $hms1_{G}$; $hms2_{N}$ gametic
397 incompatibility. Moreover, pollen viability in IL-G and IL-Ns with the genotype $hms1_{GN}$;
398 $hms2_{NN}$ is much lower than the 50% expected for gametic expression of hybrid male
399 sterility (Table 5), consistent with over-transmission of *M. guttatus hms1* alleles into
400 pollen. Note that if these two TRD mechanisms – $hms1_{G}$; $hms2_{N}$ gamete sterility and
401 over-transmission of *M. guttatus hms1* alleles – counteract each other in F_1 hybrids and in
402 doubly heterozygous ILs, it could explain why their progeny carry *hms1* alleles in
403 roughly Mendelian proportions (Table 2, Figure S1). Consistent with this idea, backcross

bioRxiv preprint doi: https://doi.org/10.1101/150854; this version posted June 16, 2017. The copyright holder for this preprint (which was not certified by peer review) is the author/funder, who has granted bioRxiv a license to display the preprint in perpetuity. It is made available under aCC-BY-ND 4.0 International license.

404 progeny of doubly heterozygous ILs are most often products of the *hms1*$_G$; *hms2*$_G$ gamete
405 type (Table 4).
406 Additionally, a genetically distinct hybrid incompatibility appears to affect
407 transmission of *hms1* against an *M. nasutus* genetic background. Self-fertilization of a
408 doubly heterozygous IL-N individual produces no *M. guttatus* homozygotes at the *hms1*
409 locus (Table 2), a genotype expected to appear in a quarter of the progeny (IL-N F_2 N =
410 200, expected frequency = 50). When instead this same doubly heterozygous IL-N
411 genotype is crossed to IM62 (in either direction), progeny homozygous for *M. guttatus*
412 alleles at *hms1* are recovered (Table S3). Note that selfing the doubly heterozygous IL-N
413 produces offspring with isogenic *M. nasutus* genetic backgrounds, whereas the backcross
414 to IM62 results in progeny with genetic backgrounds that are F_1-like. Taken together,
415 these results suggest that the *hms1* region is involved in yet another hybrid
416 incompatibility. This one causes lethality in hybrids that are homozygous for *M. guttatus*
417 alleles at *hms1* (or linked loci) and homozygous for *M. nasutus* alleles at one or more
418 unlinked loci.
419 By scoring genotype frequencies in the progeny of reciprocal backcrosses
420 involving the doubly heterozygous ILs (*hms1*$_{GN}$; *hms2*$_{GN}$), it is possible to track which
421 two-locus *hms1-2* meiotic products are transmitted through pollen and ovules. If we use
422 these observed two-locus gametic allele frequencies (instead of assuming equal
423 proportions of the four two-locus gamete types) to calculate expected genotype
424 frequencies in the selfed progeny of doubly heterozygous ILs (i.e., IL-F_2 populations), the
425 resulting values do not significantly differ from observed proportions (Table 2, Table 4).
426 To fully account for observed genotype frequencies in the IL-N F_2, it is also necessary to
427 assume complete lethality of *M. guttatus* homozygotes at *hms1* (Table 2; note that this
428 hybrid lethality is not reflected in IL backcross allele frequencies because progeny do not
429 carry the requisite *M. nasutus* genetic background for expression of the incompatibility).
430 In summary, we have identified at least three sources of *hms1-hms2* TRD in *M.*
431 *nasutus-M. guttatus* F_2 hybrids: 1) under-transmission of pollen and, to a lesser extent,
432 ovules that carry an *M. guttatus* allele at *hms1* in combination with an *M. nasutus* allele at
433 *hms2*, presumably due to gametic inviability, 2) over-transmission of *M. guttatus* alleles
434 at *hms1*, an effect that occurs through males and females, and does not depend on genetic

bioRxiv preprint doi: https://doi.org/10.1101/150854; this version posted June 16, 2017. The copyright holder for this preprint (which was not certified by peer review) is the author/funder, who has granted bioRxiv a license to display the preprint in perpetuity. It is made available under aCC-BY-ND 4.0 International license.

435 background, and 3) hybrid lethality in individuals homozygous for *M. guttatus* alleles at
436 *hms1* (and linked genomic regions) in combination with *M. nasutus* homozygosity at one
437 or more unlinked loci.
438
439 **Fine-mapping TRD**
440 In previous (Sweigart and Flagel 2015) and ongoing efforts to fine-map *hms1* and *hms2*,
441 we identified a small subset of SF5-IM62 F_2 hybrids that were recombinant for one or
442 both sets of *hms* flanking markers. With the goal of genetically mapping TRD in both
443 regions, we self-fertilized these recombinants to generate F_3 progeny and examined
444 genotype frequencies at both sets of flanking markers (Figures 3 and 4). We reasoned that
445 TRD in the F_3 progeny should only be observable if the causal locus is heterozygous in
446 the F_2 parent. If, instead, the TRD-causing locus is homozygous (for either *M. guttatus* or
447 M. *nasutus* alleles), loci in the adjacent heterozygous region should segregate in a
448 Mendelian fashion.
449 As in the IL crosses, patterns of *hms2*-linked TRD were consistent with the action
450 of *hms1*$_G$; *hms2*$_N$ gametic sterility. In this genomic region, the most extreme TRD
451 occurred in the two F_3 families that descended from F_2 hybrids with the *hms1*$_{GG}$; *hms2*$_{GN}$
452 genotype (Figure 2). Despite this general support for *hms1-hms2* gametic sterility, *hms2*-
453 linked TRD could not be unambiguously mapped to a particular genomic region (no
454 interval in Figure 2 is perfectly associated with presence/absence of TRD). Presumably,
455 genetic background in these F_2 hybrids can mask TRD associated with *hms1*$_G$; *hms2*$_N$
456 gametic sterility (*e.g.*, 28_22) or mimic it (*e.g.*, 02_66).
457 At *hms1*, the two contributors to TRD were decoupled in F_2 recombinants with *M.*
458 *guttatus* homozygotes overrepresented in some F_3 families and underrepresented in others
459 (Figure 3). As with the IL experiments, the most significant over-transmission of *M.*
460 *guttatus* alleles at *hms1* appears in the progeny of F_2 hybrids that are homozygous for *M.*
461 *nasutus* alleles at *hms2* (Figure 3, first two F_2s). This TRD phenotype maps to an 800-kb
462 region that includes *hms1*, but we have too few recombinants to determine if the hybrid
463 TRD phenotype is genetically separable from hybrid sterility. For a distinct set of *hms1*
464 F_2 recombinants, we observed a severe deficit of *M. guttatus* homozygotes among their
465 F_3 progeny (Figure 3, last six F_2 individuals), consistent with the expression of hybrid

bioRxiv preprint doi: https://doi.org/10.1101/150854; this version posted June 16, 2017. The copyright holder for this preprint (which was not certified by peer review) is the author/funder, who has granted bioRxiv a license to display the preprint in perpetuity. It is made available under aCC-BY-ND 4.0 International license.

466 lethality as seen in the IL experiments. This TRD phenotype maps to at least two
467 independent loci in the *hms1* region and is not affected by *hms2* genotype, suggesting a
468 distinct genetic basis for this hybrid incompatibility.
469

470 **TRD at *hms1* within *M. guttatus***

471 To investigate whether *hms1*-linked TRD is a strictly hybrid phenomenon or also occurs
472 within *M. guttatus*, we generated reciprocal F_2 progeny between IM62 and IM767. These
473 two inbred lines carry distinct alleles at *hms1* and show very different patterns of
474 variation in the surrounding genomic region. The IM62 line carries an incompatible,
475 hybrid sterility-causing *hms1* allele embedded within a distinctive, 320-kb haplotype,
476 whereas IM767 carries a compatible (*i.e.*, non-sterility causing) allele at *hms1* and typical
477 levels of nucleotide variation in the region (Sweigart and Flagel 2015). Because genotype
478 frequencies at *hms1* did not differ significantly between reciprocal F_2 populations (data
479 not shown), we pooled data from both directions of the cross. We observed modest, but
480 significant TRD at *hms1* with an excess of IM62 homozygotes (frequency of IM62
481 homozygotes to heterozygotes to IM767 homozygotes: expected 0.25:0.5:0.25, observed
482 00.27:0.54:0.19, $X^2 = 6.479$, d.f. = 2, $P = 0.0027$, $N = 582$). However, the bias in allelic
483 transmission toward IM62 was not significant (frequency of IM62:IM767 alleles:
484 expected 0.5:0.5, observed 0.54:0.46, $X^2 = 0.151$, d.f. = 1, $P < 0.151$, $N = 582$) and
485 genotype frequencies did not significantly differ from the expectation given the allele
486 frequencies ($X^2 = 2.025$, d.f. = 2, $P = 2.025$, $N = 582$). To further investigate the
487 mechanism of *hms1*-linked TRD, we performed reciprocal backcrosses using IM62 and
488 IM767. However, unlike in the IM62-IM767 F_2 hybrids, all four backcross populations
489 exhibited nearly perfect Mendelian ratios (expected 0.50:0.50; F_1 x IM62 = 0.50:0.50, N
490 = 279; F_1 x IM767 = 0.50:0.50, $N = 281$; IM62 x F_1 = 0.51:0.49, $N = 189$; IM767 x F_1 =
491 0.49:0.51, $N = 188$). These results suggest there is little to no transmission bias favoring
492 the *hms1* incompatibility allele or the associated 320-kb haplotype within the Iron
493 Mountain population.

494 Finally, we wanted to investigate if the presence of *M. nasutus* alleles at *hms2*
495 increases the transmission bias of IM62 at *hms1* – even in an otherwise *M. guttatus*
496 genetic background. To address this question, we examined genotype frequencies in the

bioRxiv preprint doi: https://doi.org/10.1101/150854; this version posted June 16, 2017. The copyright holder for this preprint (which was not certified by peer review) is the author/funder, who has granted bioRxiv a license to display the preprint in perpetuity. It is made available under aCC-BY-ND 4.0 International license.

497 reciprocal backcross progeny of individuals that were heterozygous IM62/IM767 at *hms1*
498 and segregating for an *M. nasutus* introgression at *hms2* (against an otherwise IM62-
499 IM767 F_2 genetic background; Figure S2). Indeed, extreme TRD at *hms1* (*i.e.*, bias
500 toward the IM62 allele > 70%) was only observed in the backcross progeny of one
501 individual (08_60) that was also homozygous for *M. nasutus* alleles at *hms2* (Table 6).
502 These results suggest that over-transmission of the IM62 allele at *hms1*, which appears to
503 require *M. nasutus* alleles at *hms2*, may occur exclusively in hybrids.
504
505 **DISCUSSION**
506
507 Transmission ratio distortion is commonly observed among hybrid offspring of recently
508 diverged species, but the evolutionary significance is not always clear. In this study, we
509 identified multiple contributors to hybrid TRD in genomic regions linked to two *Mimulus*
510 hybrid sterility loci *hms1* and *hms2*, revealing a fine-scale complexity reminiscent of
511 several previously characterized hybrid incompatibilities (Davis and Wu 1996; Long et
512 al. 2008; Yang et al. 2012; Kubo et al. 2016b). We have discovered that hybrid
513 transmission bias is caused, in part, by gametic action of the *hms1-hms2* incompatibility
514 itself. However, the effects of the gametic hybrid sterility are partially obscured by an
515 opposing (and currently unknown) mechanism that results in over-transmission of the *M.*
516 *guttatus hms1* incompatibility allele in certain hybrid genetic backgrounds. In addition,
517 our genetic analyses uncovered an independent hybrid lethality system with at least two
518 incompatibility loci tightly linked to *hms1*. Strikingly, we found no evidence of biased
519 transmission of the *hms1* incompatibility allele within *M. guttatus*, providing little
520 support for selfish evolution as the cause of a recent, partial sweep at *hms1* (Sweigart and
521 Flagel 2015). Instead, it appears that TRD at *hms1* and *hms2* might occur exclusively in
522 hybrids.
523
524 **Gametic action of *hms1-hms2* hybrid incompatibility**
525 Our finding that the $hms1_G$; $hms2_N$ gamete type is severely under-transmitted in six of the
526 eight backcrosses involving doubly heterozygous ILs ($hms1_{GN}$; $hms2_{GN}$) is strong
527 evidence of gametic action of the incompatibility. This result runs counter to our previous

bioRxiv preprint doi: https://doi.org/10.1101/150854; this version posted June 16, 2017. The copyright holder for this preprint (which was not certified by peer review) is the author/funder, who has granted bioRxiv a license to display the preprint in perpetuity. It is made available under aCC-BY-ND 4.0 International license.

528 interpretation of the finding that pollen viability is reduced from the F_1 to F_2 generation,
529 which seemed to suggest a diploid (sporophytic) genetic basis for the *hms1-hms2*
530 incompatibility (Sweigart et al. 2006). In general, for a hybrid incompatibility that affects
531 the gametophyte, sterility is expected to be less severe in the F_2 generation due to the
532 inviability of recombinant F_1 gametes and regeneration of parental combinations.
533 However, in this case, it appears that removal of $hms1_G$; $hms2_N$ F_1 gametes is somewhat
534 balanced by over-transmission of *M. guttatus* alleles at *hms1*. Moreover, incomplete
535 penetrance of F_1 hybrid gametic sterility (*i.e*., some $hms1_G$; $hms2_N$ gametes do contribute
536 to the F_2 generation, see Table 4) produces a small fraction of F_2 hybrids that are
537 completely sterile because they are homozygous for incompatible alleles (*i.e*., $hms1_{GG}$;
538 $hms2_{NN}$).

539 As an independent line of evidence for gametic expression of the *hms1-hms2*
540 incompatibility, it is apparently difficult to introgress *M. nasutus hms2* alleles into an *M.*
541 *guttatus* genetic background. In the BG_4-NIL population (generated by four rounds of
542 backcrossing using IM62 as the pollen donor; see Methods from this study and Fishman
543 and Willis 2005), only 2.8% of individuals (5/175) are heterozygous at MgSTS45, a
544 marker ~2 cM from *hms2* (L. Fishman, unpublished results). This level of distortion is
545 notable: of the 194 markers genotyped in this BG_4 population, only four of them show
546 lower heterozygosity and three of those map near a meiotic drive locus that strongly
547 favors the *M. guttatus* allele (Fishman and Saunders 2008). In the BN_4 population
548 (generated by four rounds of backcrossing with SF5 as the pollen donor), heterozygous
549 introgressions at MgSTS45 are much more common, occurring in 10% of individuals (18
550 of 181). This result is not unexpected given that *M. guttatus* alleles at *hms2* are perfectly
551 compatible with *M. nasutus* alleles at *hms1*.

552 Unlike in animals, hybrid incompatibilities in plants are often gametic
553 (Morishima et al. 1991; Koide et al. 2008b; Leppala et al. 2013). Based on his studies of
554 hybrid sterility between the *indica* and *japonica* varieties of *Oryza sativa*, Oka (1974)
555 first suggested that defects in pollen development might be caused by loss-of-function
556 alleles at duplicate genes (Oka 1974). Indeed, two cases of this duplicate gametic lethal
557 model have now been demonstrated at the molecular level (Mizuta et al. 2010; Yamagata
558 et al. 2010). For *Mimulus hms1* and *hms2*, there's no evidence that gene duplicates are

bioRxiv preprint doi: https://doi.org/10.1101/150854; this version posted June 16, 2017. The copyright holder for this preprint (which was not certified by peer review) is the author/funder, who has granted bioRxiv a license to display the preprint in perpetuity. It is made available under aCC-BY-ND 4.0 International license.

559 involved (Sweigart and Flagel 2015), but a similar pattern of hybrid sterility is expected
560 to result from a two-locus hybrid incompatibility between any genes expressed in the
561 gametophyte. Additionally, the fact that the *hms1-hms2* incompatibility seems to affect
562 both the male and female gametophyte (the *hms1*$_G$; *hms2*$_N$ gamete type is under-
563 transmitted through both sexes) is consistent with our finding that these loci contribute to
564 both hybrid male sterility and hybrid female sterility (Sweigart et al. 2006). Gametic
565 hybrid incompatibilities that affect the fertility of both sexes have also been discovered in
566 tomato, rice, and *Arabidopsis* (Rick 1966; Koide et al. 2008a; Leppala et al. 2013),
567 though they are apparently less common than those that act in only one sex (Morishima et
568 al. 1991; Koide et al. 2008b)
569
570 **Additional sources of transmission ratio distortion**
571 Our fine-scale dissection of TRD at *hms1* and *hms2* provides insight into genomic
572 differentiation between closely related *Mimulus* species and reveals a potentially complex
573 genetic basis for hybrid dysfunction. In other systems, fine-mapping has often revealed
574 multiple, tightly linked hybrid incompatibility loci that show independent effects (Wu
575 and Davis 1993; Kubo et al. 2016a; Simon et al. 2016) or epistasis (Long et al. 2008;
576 Yang et al. 2012; Kubo et al. 2016b). In one particularly complex example from *indica*
577 and *japonica*, fine-mapping revealed two tightly linked genes involved in independent
578 two-locus pollen killer systems (Kubo et al. 2016b). Because of this tight linkage, pollen
579 killing had initially appeared to be caused by a single, three-locus interaction (Kubo *et al.*
580 2008). Remarkably, both of these pollen killer systems involve interactions between
581 sporophytic and gametophytic genes, as well as additional modifier loci (Kubo et al.
582 2016b). The picture emerging from such studies is one of hybrid sterility regulated by
583 multiple, interconnected molecular networks, potentially involving many genes.
584 A key question for *hms1* and *hms2* is whether the same genes cause the gametic
585 incompatibility and transmission bias of *M. guttatus* at *hms1*. The latter is particularly
586 strong when *hms2* is homozygous for *M. nasutus* alleles (Table 3, Figure S1), suggesting
587 it might be caused by an interaction between the two loci. Additionally, the presence of
588 *hms2*$_{NN}$ also appeared to unleash severe *hms1* TRD in one of the two IM62-IM767 F_2
589 populations in which it was present (Table 6), suggesting *hms2* might be necessary but

bioRxiv preprint doi: https://doi.org/10.1101/150854; this version posted June 16, 2017. The copyright holder for this preprint (which was not certified by peer review) is the author/funder, who has granted bioRxiv a license to display the preprint in perpetuity. It is made available under aCC-BY-ND 4.0 International license.

590 not sufficient for *hms1* TRD. On the other hand, over-transmission of *hms1*$_G$ does not
591 seem to absolutely require *hms2*$_{NN}$ (*e.g.*, we observed 62% transmission of *hms1*$_G$ in *M.*
592 *nasutus* x IL-G$_{GN;GG}$, Table 3), which might argue against its direct involvement. Indeed,
593 for the IL-Gs, there is a bias toward *hms1*$_G$ in all backcross populations except those
594 involving doubly heterozygous IL parents (*i.e.*, *hms1*$_{GN}$; *hms2*$_{GN}$), which, because they
595 express the *hms1*$_G$; *hms2*$_N$ gametic inviability, might obscure additional sources of *hms1*
596 TRD. Going forward, additional rounds of high-resolution fine-mapping will be needed
597 to pinpoint the causal genes and determine if *Mimulus* hybrid sterility and TRD are
598 genetically separable. Such efforts in rice have been successful in disentangling the
599 complex phenotypic effects of linked hybrid sterility loci (*e.g.*, (Kubo et al. 2016a).
600 Identifying the molecular genetic basis of *hms1* TRD might also provide insight
601 into its mechanisms. Because the bias toward *M. guttatus* alleles at *hms1* occurs through
602 both males and females, the simplest single explanation is a gamete killing system that
603 affects pollen and seeds. Alternatively, it is possible that independent mechanisms (and
604 genetic loci) cause sex-specific TRD, such as pollen competition in males (*e.g.*, (Fishman
605 et al. 2008)) and meiotic drive in females (*e.g.*, (Fishman and Saunders 2008). Whatever
606 the cause, over-transmission of *hms1*$_G$ is apparently exacerbated by *M. nasutus* alleles at
607 *hms2* to the point of overwhelming the effects of the *hms1*$_G$; *hms2*$_N$ gametic
608 incompatibility. Indeed, the direction of TRD in the backcross progeny of *hms1*$_{GN}$;
609 *hms2*$_{NN}$ ILs is counterintuitive: because of the *hms1*$_G$; *hms2*$_N$ gametic incompatibility,
610 one expects transmission bias to be toward *M. nasutus* alleles. Instead, we observed
611 exactly the opposite, namely, strong transmission bias toward *M. guttatus* at *hms1*. This
612 finding might help explain < 50% pollen inviability in ILs with the genotype *hms1*$_{GN}$;
613 *hms2*$_{NN}$. If *hms1*$_G$ alleles are highly overrepresented in pollen of such individuals due to
614 gamete killing or some other mechanism, the gametic incompatibility will be expressed
615 more often than expected under Mendelian inheritance. However, to explain the bias
616 toward *M. guttatus* alleles in the backcross progeny, the gamete killing phenotype has to
617 be stronger than the gametic incompatibility. In other words, some fraction of *hms1*$_G$;
618 *hms2*$_N$ gametes must survive – and in greater numbers than *hms1*$_N$; *hms2*$_N$ gametes – to
619 form zygotes. Clarifying the role of *hms2* in *hms1* TRD, and whether it acts through the

bioRxiv preprint doi: https://doi.org/10.1101/150854; this version posted June 16, 2017. The copyright holder for this preprint (which was not certified by peer review) is the author/funder, who has granted bioRxiv a license to display the preprint in perpetuity. It is made available under aCC-BY-ND 4.0 International license.

620 diploid sporophyte or haploid gametophyte, will be an important step toward
621 understanding the mechanistic basis of hybrid distortion.
622 Surprisingly, our crossing experiments revealed at least two additional hybrid
623 incompatibility loci linked to *hms1*. These loci, which contribute to TRD in the IL-Ns,
624 appear to cause hybrid inviability and involve recessive alleles from both *Mimulus*
625 species: against an *M. nasutus* genetic background, the *hms1* region cannot be made
626 homozygous for *M. guttatus* alleles. The precise locations of these hybrid lethality loci
627 are not yet known (Figure 3), but both potentially overlap with the 320-kb haplotype
628 associated with the *hms1* incompatibility allele (Sweigart and Flagel 2015). This nearly
629 invariant haplotype, which includes 30 genes, has recently risen to intermediate
630 frequency in the Iron Mountain population of *M. guttatus*. The fact that multiple hybrid
631 incompatibility loci are associated with this sweeping haplotype suggest that natural
632 selection within a single population might have profound consequences for reproductive
633 isolation between *Mimulus* species.
634

635 **Implications for the evolution of hybrid sterility in *Mimulus***

636 An emerging theme in speciation genetics is that selfish evolution within species might
637 be a major driver of hybrid incompatibilities. Decades of genetic analysis have provided a
638 detailed mechanistic understanding of classic segregation distorters within *Drosophila*
639 and mouse species (see (Presgraves 2008), and more recent studies have shown that
640 hybrid sterility and hybrid TRD can be caused by the same genes (Phadnis and Orr
641 2009a; Zhang et al. 2015). However, very few studies have directly linked these two ends
642 of the spectrum, testing whether incompatibility alleles act as selfish genetic elements
643 within species. In one recent exception, Case *et al*. (2016) showed population genomic
644 evidence for coevolution between a selfish cytoplasmic male sterility (CMS) gene and a
645 nuclear restorer of fertility (*Rf* locus) within the Iron Mountain population of *M. guttatus*
646 (Case et al. 2016). These same two loci also cause hybrid male sterility between *M.*
647 *guttatus* and *M. nasutus*, suggesting that intragenomic conflict within Iron Mountain
648 contributes to interspecific reproductive barriers.
649 Direct evidence for selfish evolution is missing from any of the hybrid gamete
650 eliminators that have been cloned in rice (Long et al. 2008; Kubo et al. 2011; Yang et al.

bioRxiv preprint doi: https://doi.org/10.1101/150854; this version posted June 16, 2017. The copyright holder for this preprint (which was not certified by peer review) is the author/funder, who has granted bioRxiv a license to display the preprint in perpetuity. It is made available under aCC-BY-ND 4.0 International license.

651 2012; Kubo et al. 2016a; Kubo et al. 2016b; Yu et al. 2016). In most of these hybrid
652 sterility systems, patterns of molecular variation at the causal genes in *japonica*, *indica*,
653 and their wild ancestor *Oryza rufipogon* suggest that hybrid incompatibility alleles may
654 never have expressed their killing phenotypes within species (*e.g.*, (Long et al. 2008;
655 Yang et al. 2012),; also see (Sweigart and Willis 2012). In plants, it is also important to
656 consider that even if gamete eliminators do arise within species and evolve selfishly to
657 bias their own transmission, they might do so without any cost to individual fitness (Rick
658 1966). Especially for pollen killers, a sufficient number of viable pollen grains might still
659 remain to fertilize all available ovules. Under a scenario of selfish evolution with no
660 fitness costs, there is no conflict and, thus, no mechanism for generating hybrid
661 incompatibilities.

662 Despite evidence for a recent selective sweep of the *hms1*-associated haplotype in
663 the Iron Mountain population (Sweigart and Flagel 2015), our crossing experiments
664 suggest there is no transmission bias favoring the IM62 *hms1* incompatibility allele. One
665 caveat to this finding is that TRD at *hms1* might vary in different genetic backgrounds;
666 even if there is no transmission bias between the IM62 and IM767 *hms1* alleles, TRD
667 might occur in other heterozygous combinations. Alternatively, Iron Mountain
668 individuals, including IM62 and IM762, might carry suppressors at *hms2*. However,
669 given the recentness of the *hms1*-associated sweep (i.e. ~63 generations old; Sweigart and
670 Flagel 2015), it seems unlikely that there has been sufficient time for a suppressor to
671 evolve. Instead, *M. guttatus* from Iron Mountain and elsewhere may carry a "permissive"
672 allele at *hms2* that allowed the evolution of the IM62 *hms1* variant without it expressing
673 any transmission bias or sterility. Consistent with this idea, the incompatibility allele at
674 *hms2* seems to be specific to *M. nasutus* (Sweigart et al. 2007), indicating this species
675 likely carries the derived allele. Thus, instead of being driven by selfish evolution within
676 *M. guttatus*, it appears that TRD at *hms1* is limited only to hybrids. These findings leave
677 open the possibility that *hms1* evolution within Iron Mountain may have been driven by
678 ecological adaptation. Further molecular characterization of these hybrid incompatibility
679 loci and direct investigations of the fitness effects of alternative alleles at *hms1* will be
680 important steps toward identifying the evolutionary causes of this reproductive barrier.
681

bioRxiv preprint doi: https://doi.org/10.1101/150854; this version posted June 16, 2017. The copyright holder for this preprint (which was not certified by peer review) is the author/funder, who has granted bioRxiv a license to display the preprint in perpetuity. It is made available under aCC-BY-ND 4.0 International license.

682 **ACKNOWLEDGEMENTS**
683 We thank Lila Fishman for sharing her BG_4 and BN_4 NILs and for valuable discussions.
684 We are also grateful to Matt Zuellig who made thoughtful comments on an earlier draft,
685 which improved the manuscript. We are especially indebted to Taylor Harrell and Rachel
686 Hughes for expert greenhouse care and genotyping assistance. This work was supported
687 by a National Science Foundation grant DEB-1350935 and funds from the University of
688 Georgia Research Foundation to ALS.
689
690
691 **REFERENCES**
692
693 Barreau, C., E. Benson, E. Gudmannsdottir, F. Newton, and H. White-Cooper. 2008.
694 Post-meiotic transcription in *Drosophila* testes. Development 135:1897-
695 1902.
696 Brandvain, Y., A. M. Kenney, L. Flagel, G. Coop, and A. L. Sweigart. 2014. Speciation
697 and introgression between *Mimulus nasutus* and *Mimulus guttatus*. PLoS
698 genetics 10:e1004410.
699 Braun, R. E., R. R. Behringer, J. J. Peschon, R. L. Brinster, and R. D. Palmiter. 1989.
700 Genetically haploid spermatids are phenotypically diploid. Nature 337:373-
701 376.
702 Burt, A. and R. Trivers. 2006. Genes in conflict: the biology of selfish genetic
703 elements. Harvard University Press, Cambridge, Massachusetts.
704 Cameron, D. R. and R. M. Moav. 1957. Inheritance in *Nicotiana tabacum* XXVII. Pollen
705 killer, an alien genetic locus inducing abortion of microspores not carrying
706 it.326-335.
707 Case, A. L., F. R. Finseth, C. M. Barr, and L. Fishman. 2016. Selfish evolution of
708 cytonuclear hybrid incompatibility in *Mimulus*. Proceedings. Biological
709 sciences / The Royal Society 283.
710 Case, A. L. and J. H. Willis. 2008. Hybrid male sterility in *Mimulus* (Phrymaceae) is
711 associated with a geographically restricted mitochondrial rearrangement.
712 Evolution; international journal of organic evolution 62:1026-1039.
713 Christie, P. and M. R. Macnair. 1987. The distribution of postmating reproductive
714 isolating genes in populations of the yellow monkey flower, *Mimulus*
715 *guttatus*. Evolution; international journal of organic evolution 41:571-578.
716 Crespi, B. and P. Nosil. 2013. Conflictual speciation: species formation via genomic
717 conflict. Trends in ecology & evolution 28:48-57.
718 Davis, A. W. and C.-I. Wu. 1996. The broom of the sorcerer's apprentice: the fine
719 structure of a chromosomal region causing reproductive isolation between
720 two sibling species of *Drosophila*. Genetics 143:1287-1298.
721 Diaz, A. and M. R. Macnair. 1999. Pollen tube competition as a mechanism of
722 prezygotic reproductive isolation between *Mimulus nasutus* and its presumed
723 progenitor *M. guttatus*. The New phytologist 144:471-478.

bioRxiv preprint doi: https://doi.org/10.1101/150854; this version posted June 16, 2017. The copyright holder for this preprint (which was not certified by peer review) is the author/funder, who has granted bioRxiv a license to display the preprint in perpetuity. It is made available under aCC-BY-ND 4.0 International license.

724 Fishman, L., J. Aagaard, and J. C. Tuthill. 2008. Toward the evolutionary genomics of
725 gametophytic divergence: patterns of transmission ratio distortion in
726 monkeyflower (*Mimulus*) hybrids reveal a complex genetic basis for
727 conspecific pollen precedence. Evolution; international journal of organic
728 evolution 62:2958-2970.
729 Fishman, L. and A. Saunders. 2008. Centromere-associated female meiotic drive
730 entails male fitness costs in monkeyflowers. Science 322:1559-1561.
731 Fishman, L., A. L. Sweigart, A. M. Kenney, and S. Campbell. 2014. Major quantitative
732 trait loci control divergence in critical photoperiod for flowering between
733 selfing and outcrossing species of monkeyflower (*Mimulus*). The New
734 phytologist 201:1498-1507.
735 Fishman, L. and J. H. Willis. 2005. A novel meiotic drive locus almost completely
736 distorts segregation in *Mimulus* (monkeyflower) hybrids. Genetics 169:347-
737 353.
738 Frank, S. A. 1991. Divergence of meiotic drive-suppression systems as an
739 explanation for sex-biased hybrid sterility and inviability. Evolution;
740 international journal of organic evolution 45:262-267.
741 Gossmann, T. I., D. Saleh, M. W. Schmid, M. A. Spence, and K. J. Schmid. 2016.
742 Transcriptomes of plant gametophytes have a higher proportion of rapidly
743 evolving and young genes than sporophytes. Molecular biology and evolution
744 33:1669-1678.
745 Gossmann, T. I., M. W. Schmid, U. Grossniklaus, and K. J. Schmid. 2014. Selection-
746 driven evolution of sex-biased genes is consistent with sexual selection in
747 *Arabidopsis thaliana*. Molecular biology and evolution 31:574-583.
748 Hurst, L. D. and A. Pomiankowski. 1991. Causes of sex ratio bias may account for
749 unisexual sterility in hybrids: a new explanation of Haldane's Rule and
750 related phenomena. Genetics 128:841-858.
751 Johnson, N. A. 2010. Hybrid incompatibility genes: remnants of a genomic
752 battlefield? Trends in genetics : TIG 26:317-325.
753 Kenney, A. M. and A. L. Sweigart. 2016. Reproductive isolation and introgression
754 between sympatric *Mimulus* species. Molecular ecology 25:2499-2517.
755 Koide, Y., M. Ikenaga, N. Sawamura, D. Nishimoto, K. Matsubara, K. Onishi, A.
756 Kanazawa, and Y. Sano. 2008a. The evolution of sex-independent
757 transmission ratio distortion involving multiple allelic interactions at a single
758 locus in rice. Genetics 180:409-420.
759 Koide, Y., K. Onishi, A. Kanazawa, and Y. Sano. 2008b. Genetics of speciation in rice.
760 Rice Biology in the Genomics Era. Springer, Verlag Berlin Heidelberg.
761 Kubo, T. 2013. Genetic mechanisms of postzygotic reproductive isolation: An
762 epistatic network in rice. Breed Sci 63:359-366.
763 Kubo, T., T. Takashi, M. Ashikari, A. Yoshimura, and N. Kurata. 2016a. Two tightly
764 linked genes at the hsa1 locus cause both F1 and F2 hybrid sterility in rice.
765 Molecular plant 9:221-232.
766 Kubo, T., A. Yoshimura, and N. Kurata. 2011. Hybrid male sterility in rice is due to
767 epistatic interactions with a pollen killer locus. Genetics 189:1083-1092.

bioRxiv preprint doi: https://doi.org/10.1101/150854; this version posted June 16, 2017. The copyright holder for this preprint (which was not certified by peer review) is the author/funder, who has granted bioRxiv a license to display the preprint in perpetuity. It is made available under aCC-BY-ND 4.0 International license.

768 Kubo, T., A. Yoshimura, and N. Kurata. 2016b. Pollen killer gene S35 function
769 requires interaction with an activator that maps close to S24, another pollen
770 killer gene in rice. G3 6:1459-1468.
771 Leppala, J., F. Bokma, and O. Savolainen. 2013. Investigating incipient speciation in
772 *Arabidopsis lyrata* from patterns of transmission ratio distortion. Genetics
773 194.
774 Loegering, W. Q. and E. R. Sears. 1963. Distorted inheritance of stem-rust resistance
775 of Timstein wheat caused by a pollen-killing gene. Canadian Journal of
776 Genetics and Cytology 5:65-72.
777 Long, Y., L. Zhao, B. Niu, Su, J., H. Wu, Y. Chen, Zhang, Q., J. Guo, C. Zhuang, M. Mei, and
778 J. Xia. 2008. Hybrid male sterility in rice controlled by interaction between
779 divergent alleles of two adjacent genes. PNAS 105:18871-18876.
780 Lynch, M. and A. G. Force. 2000. The origin of interspecific genomic incompatibility
781 via gene duplication. American Naturalist 156:590-605.
782 Maheshwari, S. and D. A. Barbash. 2011. The genetics of hybrid incompatibilities.
783 Annu Rev Genet 45:331-355.
784 Martin, N. H. and J. H. Willis. 2007. Ecological divergence associated with mating
785 system causes nearly complete reproductive isolation between sympatric
786 *Mimulus* species. Evolution; international journal of organic evolution 61:68-
787 82.
788 Martin, N. H. and J. H. Willis. 2010. Geographical variation in postzygotic isolation
789 and its genetic basis within and between two *Mimulus* species. Philosophical
790 transactions of the Royal Society of London. Series B, Biological sciences
791 365:2469-2478.
792 McDermott, S. R. and M. A. Noor. 2010. The role of meiotic drive in hybrid male
793 sterility. Philosophical transactions of the Royal Society of London. Series B,
794 Biological sciences 365:1265-1272.
795 Mizuta, Y., Y. Harushima, and N. Kurata. 2010. Rice pollen hybrid incompatibility
796 caused by reciprocal gene loss of duplicated genes. PNAS 107:20417-20422.
797 Morishima, H., Y. Sano, and H.-I. Oka. 1991. Sterility barriers developed between and
798 within taxa. Pp. 159-166. Evolutionary studies in rice.
799 Oka, H.-I. 1974. Analysis of genes controlling F, sterility in rice by the use of isogenic
800 lines. Genetics 77:521-534.
801 Ouyang, Y. and Q. Zhang. 2013. Understanding reproductive isolation based on the
802 rice model. Annual review of plant biology 64:111-135.
803 Phadnis, N. and H. A. Orr. 2009a. A single gene causes both male sterility and
804 segregation distortion in *Drosophila* hybrids. Science 323:376-378.
805 Phadnis, N. and H. A. Orr. 2009b. A Single Gene Causes Both Male Sterility and
806 Segregation Distortion in *Drosophila* HybridsA Single Gene Causes Both Male
807 Sterility and Segregation Distortion in Drosophila Hybrids. Science 323:376-
808 378.
809 Presgraves, D. 2008. Drive and sperm: the evolution and genetics of male meiotic
810 drive.471-506.
811 Presgraves, D. C. 2010. The molecular evolutionary basis of species formation.
812 Nature reviews. Genetics 11:175-180.

bioRxiv preprint doi: https://doi.org/10.1101/150854; this version posted June 16, 2017. The copyright holder for this preprint (which was not certified by peer review) is the author/funder, who has granted bioRxiv a license to display the preprint in perpetuity. It is made available under aCC-BY-ND 4.0 International license.

813 Rick, C. M. 1966. Abortion of male and female gametes in the tomato determined by
814 allelic interaction. Genetics 53:85-96.
815 Rutley, N. and D. Twell. 2015. A decade of pollen transcriptomics. Plant Reprod
816 28:73-89.
817 Sano, Y. 1990. The genic nature of gamete eliminator in rice. Genetics 125:183-191.
818 Schluter, D. and G. L. Conte. 2009. Genetics and ecological speciation PNAS
819 106:9955-9962.
820 Simon, M., S. Durand, N. Pluta, N. Gobron, L. Botran, A. Ricou, C. Camilleri, and F.
821 Budar. 2016. Genomic conflicts that cause pollen mortality and raise
822 reproductive barriers in *Arabidopsis thaliana*. Genetics 203:1353-1367.
823 Sweigart, A. L., L. Fishman, and J. H. Willis. 2006. A simple genetic incompatibility
824 causes hybrid male sterility in *Mimulus*. Genetics 172:2465-2479.
825 Sweigart, A. L. and L. E. Flagel. 2015. Evidence of natural selection acting on a
826 polymorphic hybrid incompatibility locus in *Mimulus*. Genetics 199:543-554.
827 Sweigart, A. L., A. R. Mason, and J. H. Willis. 2007. Natural variation for a hybrid
828 incompatibility between two species of *Mimulus*. Evolution; international
829 journal of organic evolution 61:141-151.
830 Sweigart, A. L. and J. H. Willis. 2003. Patterns of nucleotide diversity in two species
831 of *Mimulus* are affected by mating system and asymmetric introgression.
832 Evolution; international journal of organic evolution 57:2490-2506.
833 Sweigart, A. L. and J. H. Willis. 2012. Molecular evolution and genetics of postzygotic
834 reproductive isolation in plants. F1000 biology reports 4:23.
835 Tao, Y., D. L. Hartl, and C. C. Laurie. 2001. Sex-ratio segregation distortion associated
836 with reproductive isolation in *Drosophila*Sex-ratio segregation distortion
837 associated with reproductive isolation in Drosophila. PNAS 98:13183-13188.
838 Vickery, R. K. J. 1978. Case studies in the evolution of species complexes in *Mimulus*.
839 Evolutionary Biology 11:405-507.
840 Walbot, V. and M. M. Evans. 2003. Unique features of the plant life cycle and their
841 consequences. Nature reviews. Genetics 4:369-379.
842 Werth, C. R. and M. D. Windham. 1991. A model for divergent, allopatric speciation
843 of polyploid pteridophytes resulting from silencing of duplicate-gene
844 expression. Am Nat 137:515-526.
845 Wu, C.-I. and A. W. Davis. 1993. Evolution of postmating reproductive isolation: the
846 composite nature of haldane's rule
847 and its genetic bases. Am Nat 142:187-212.
848 Wuest, S. E., K. Vijverberg, A. Schmidt, M. Weiss, J. Gheyselinck, M. Lohr, F. Wellmer,
849 J. Rahnenfuhrer, C. von Mering, and U. Grossniklaus. 2010. *Arabidopsis* female
850 gametophyte gene expression map reveals similarities between plant and
851 animal gametes. Current biology : CB 20:506-512.
852 Yamagata, Y., E. Yamamoto, K. Aya, K. T. Win, K. Doi, Sobrizal, T. Ito, H. Kanamori, J.
853 Wu, T. Matsumoto, M. Matsuoka, M. Ashikari, and A. Yoshimura. 2010.
854 Mitochondrial gene in the nuclear genome induces reproductive barrier in
855 rice. Proceedings of the National Academy of Sciences of the United States of
856 America 107:1494-1499.
857 Yang, J., X. Zhao, K. Cheng, H. Du, Y. Ouyang, J. Chen, S. Qiu, J. Huang, Y. Jiang, L. Jiang,
858 J. Ding, J. Wang, C. Xu, X. Li, and Q. Zhang. 2012. A killer-protector system

bioRxiv preprint doi: https://doi.org/10.1101/150854; this version posted June 16, 2017. The copyright holder for this preprint (which was not certified by peer review) is the author/funder, who has granted bioRxiv a license to display the preprint in perpetuity. It is made available under aCC-BY-ND 4.0 International license.

859 regulates both hybrid sterility and segregation distortion in rice. Science
860 337:1336-1340.
861 Yu, Y., Z. Zhao, Y. Shi, H. Tian, L. Liu, X. Bian, Y. Xu, X. Zheng, L. Gan, Y. Shen, C. Wang,
862 X. Yu, C. Wang, X. Zhang, X. Guo, J. Wang, H. Ikehashi, L. Jiang, and J. Wan.
863 2016. Hybrid sterility in rice (*Oryza sativa* L.) involves the tetratricopeptide
864 repeat domain containing protein. Genetics 203:1439-1451.
865 Zhang, L., T. Sun, F. Woldesellassie, H. Xiao, and Y. Tao. 2015. Sex ratio meiotic drive
866 as a plausible evolutionary mechanism for hybrid male sterility. PLoS
867 genetics 11:e1005073.
868
869
870

bioRxiv preprint doi: https://doi.org/10.1101/150854; this version posted June 16, 2017. The copyright holder for this preprint (which was not certified by peer review) is the author/funder, who has granted bioRxiv a license to display the preprint in perpetuity. It is made available under aCC-BY-ND 4.0 International license.

Table 1. Genotype and allele frequencies at *hms1* and *hms2* in an *M. nasutus*-*M. guttatus* F_2 population (N = 5487).

	Allele frequency[1]	Genotype frequency[2]	
locus	O	O	E
hms1	0.49:0.51	0.22:0.55:0.23****	0.24:0.50:0.26
hms2	0.62:0.38****	0.38:0.48:0.14	0.38:0.47:0.14

[1] Observed (O) allele frequencies are reported as *M. guttatus*:*M. nasutus* (G:N). At *hms2*, but not *hms1*, allele frequencies significantly differ from the Mendelian expectation (0.5:0.5).

[2] Observed (O) and expected (E) genotype frequencies are reported as *M. guttatus* homozygotes:heterozygotes:*M. nasutus* homozygotes (GG:GN:NN). Expected genotype frequencies shown are calculated from the random union of gametes with the observed frequencies. At *hms1*, genotypes differ significantly (P < 0.0001) from both the Mendelian expectation (0.25:0.5:0.25) and from the expectation given the random union of gametes with the observed allele frequencies. At *hms2*, genotypes differ significantly (P < 0.0001) from the Mendelian expectation but not from the expectation given the random union of gametes with the observed allele frequencies.

**** P < 0.0001 based on X^2 tests of observed frequencies versus the Mendelian expectation with 2 d. f. for genotypes and 1 d. f. for allele frequencies.

Table 2. Observed and expected genotype frequencies at *hms1* and *hms2* in F_2 hybrids and IL F_2 hybrids.

genotype *hms1*; *hms2*	F_2 (5487)[1]			IL-G F_2 (167)[2]		IL-N F_2 (200)[3]		
	E: Mendelian	E: obs allele freqs	O	O	E: backcross	O	E: backcross	E: $hms1_{GG}$ = lethal
GG; GG	0.0625	0.093	0.099	0.066	0.107	0	0.119	0
GG; GN	0.1250	0.115	0.100	0.114	0.106	0	0.069	0
GG; NN	0.0625	0.035	0.022	0.006	0.200	0	0.090	0
GN; GG	0.1250	0.191	0.208	0.174	0.176	0.185	0.193	0.241
GN; GN	0.2500	0.236	0.268	0.234	0.249	0.300	0.249	0.310
GN; NN	0.1250	0.073	0.071	0.054	0.078	0.075	0.058	0.073
NN; GG	0.0625	0.098	0.070	0.102	0.072	0.085	0.077	0.096
NN; GN	0.1250	0.121	0.117	0.180	0.133	0.225	0.151	0.188
NN; NN	0.0625	0.037	0.047	0.072	0.061	0.130	0.0740	0.092

[1]F_2 genotype counts significantly differ from the Mendelian expectation (X^2 = 389.372, d.f. = 8, P <0.0001) and from what is expected for the random union of gametes given the observed allele frequencies (see Table 1) and independent assortment at *hms1* and *hms2* (X^2 = 71.626, d.f. = 8, P <0.0001).

[2]IL-G F_2 genotype counts significantly differ from the Mendelian expectation (X^2 = 18.7910, d.f. = 8, P = 0.0160), but not from what is expected based on allelic transmission in the IL backcrosses (see Table 4, X^2 = 5.9730, d.f. = 8, P = 0.6502).

[3]IL-N F_2 genotypes significantly differ from the Mendelian expectation (X^2 = 86.4090, d.f. = 8, P <0.0001) and from what is expected based on allelic transmission in the IL backcrosses (see Table 4, X^2 = 62.0370, d.f. = 8, P <0.0001), but not from what is expected from the IL backcrosses + $hms1_{GG}$ homozygote death (X^2 = 3.5950, d.f. = 5, P =0.6090).

bioRxiv preprint doi: https://doi.org/10.1101/150854; this version posted June 16, 2017. The copyright holder for this preprint (which was not certified by peer review) is the author/funder, who has granted bioRxiv a license to display the preprint in perpetuity. It is made available under aCC-BY-ND 4.0 International license.

Table 3. Allelic transmission ratios at *hms1* and *hms2* in IL-backcross progeny.

♀[1]	♂	*hms1*; *hms2*[2]	*N*[3]	*hms1* %G[4]	*hms2* %G[5]
IL-G	G	GN; GG	101	0.56	
		GN; NN	171	0.60	
		GG; GN	163		0.53
		NN; GN	158		0.47
		GN; GN	293	0.46	0.54
IL-G	N	GN; GG	189	0.55	
		GN; NN	119	0.64*	
		GG; GN	49		0.53
		NN; GN	132		0.50
		GN; GN	232	0.52	0.54
G	IL-G	GN; GG	382	0.55	
		GN; NN	no seeds	--	
		GG; GN	120		0.86****
		NN; GN	187		0.50
		GN; GN	298	0.37***	0.67****
N	IL-G	GN; GG	636	0.62****	
		GN; NN	no seeds	--	
		GG; GN	158		0.90****
		NN; GN	187		0.52
		GN; GN	450	0.53	0.64****
IL-N	G	GN; GG	266	0.44	
		GN; NN	593	0.48	
		GG; GN	n/a		--
		NN; GN	325		0.55
		GN; GN	354	0.42*	0.59*
IL-N	N	GN; GG	211	0.48	
		GN; NN	317	0.52	
		GG; GN	n/a		--
		NN; GN	43		0.54
		GN; GN	320	0.58*	0.66****
G	IL-N	GN; GG	113	0.46	
		GN; NN	85	0.71**	
		GG; GN	n/a		--
		NN; GN	250		0.53
		GN; GN	104	0.37*	0.64*
N	IL-N	GN; GG	177	0.51	
		GN; NN	194	0.72****	
		GG; GN	n/a		--
		NN; GN	188		0.57
		GN; GN	212	0.42	0.61*

[1]Backcrosses using ILs (*M. guttatus* background = IL-G; *M. nasutus* background = IL-N) to the IM62 line of *M. guttatus* (G) and the SF5 line of *M. nasutus* (N). ♀ indicates the maternal parent and ♂ indicates the paternal parent.
[2]Two-locus genotype for *hms1* and *hms2*. GG = *M. guttatus* homozygote; GN = heterozygote; NN = *M. nasutus* homozygote.
[3]Number of progeny assessed. Two crosses were unsuccessful (labeled "no seeds") because the IL-G with the genotype $hms1_{GN}$; $hms2_{NN}$ was completely male sterile. The IL-N with the genotype $hms1_{GG}$; $hms2_{GN}$ could not be generated (see text) and is labeled "n/a."
[4]Percent *M. guttatus* (G) alleles at *hms1* transmitted to progeny from heterozygous IL parent.
[5]Percent *M. guttatus* (G) alleles at *hms2* transmitted to progeny from heterozygous IL parent.
* $P < 0.05$, ** $P < 0.01$, *** $P < 0.005$, **** $P < 0.0001$ based on X^2 tests of observed frequencies versus the Mendelian expectation.

bioRxiv preprint doi: https://doi.org/10.1101/150854; this version posted June 16, 2017. The copyright holder for this preprint (which was not certified by peer review) is the author/funder, who has granted bioRxiv a license to display the preprint in perpetuity. It is made available under aCC-BY-ND 4.0 International license.

Table 4. Two-locus transmission ratios at *hms1* and *hms2* in backcross progeny of doubly heterozygous ILs.

			hms1;hms2[3]				
♀[1]	♂	*N*[2]	G;G	G;N	N;G	N;N	*P*
IL-G	G	293	0.31	0.20	0.24	0.25	
IL-G	N	232	0.28	0.24	0.25	0.22	
IL-N	G	354	0.30	0.13	0.30	0.28	***
IL-N	N	320	0.43	0.15	0.22	0.19	****
average			0.33	0.18	0.25	0.24	
G	IL-G	298	0.32	0.05	0.35	0.28	****
N	IL-G	450	0.40	0.13	0.24	0.23	****
G	IL-N	104	0.34	0.03	0.30	0.34	****
N	IL-N	212	0.32	0.10	0.30	0.29	***
average			0.34	0.08	0.30	0.28	

[1]Backcrosses using ILs (*M. guttatus* background = IL-G; *M. nasutus* background = IL-N) to the IM62 line of *M. guttatus* (G) and the SF5 line of *M. nasutus* (N). ♀ indicates the maternal parent and ♂ indicates the paternal parent.
[2]Number of progeny assessed.
[3]Two-locus allelic combination at *hms1* and *hms2* inherited from IL parent. G = *M. guttatus* allele; N = *M. nasutus* allele.
* $P < 0.05$, ** $P < 0.01$, *** $P < 0.005$, **** $P < 0.0001$ based on X^2 tests of observed frequencies versus the Mendelian expectation.

bioRxiv preprint doi: https://doi.org/10.1101/150854; this version posted June 16, 2017. The copyright holder for this preprint (which was not certified by peer review) is the author/funder, who has granted bioRxiv a license to display the preprint in perpetuity. It is made available under aCC-BY-ND 4.0 International license.

Table 5. Pollen viability for various *hms1-2* IL genotypes.

Genetic Background	*hms1*; *hms2*	*N*[1]	PV[2]
IL-G	GG; GN	5	0.64 (0.04)
	NN; GN	16	0.79 (0.04)
	GN; GN	16	0.67 (0.06)
	GN; GG	12	0.71 (0.06)
	GN; NN	3	0.18 (0.17)
IL-N	NN; GN	15	0.88 (0.02)
	GN; GN	14	0.81 (0.03)
	GN; GG	13	0.85 (0.02)
	GN; NN	18	0.09 (0.01)

[1]Number of individuals scored.
[2]Pollen viability given as the proportion viable pollen grains per flower (for a haphazard sample of 100). PV is the average of two flowers and the number in parentheses is the standard error.

bioRxiv preprint doi: https://doi.org/10.1101/150854; this version posted June 16, 2017. The copyright holder for this preprint (which was not certified by peer review) is the author/funder, who has granted bioRxiv a license to display the preprint in perpetuity. It is made available under aCC-BY-ND 4.0 International license.

Table 6. Transmission of IM62 vs. IM767 at *hms1* varies depending on *hms2* genotype.

hms2 genotype	F_2 ID[1]	%IM62[2]	
		F_2 male	F_2 female
IM62	02_02	0.58 (74)	0.55 (64)
	02_46	0.48 (121)	0.43 (28)
	06_31	0.55 (179)	0.29 (41)
	06_70	0.55 (123)	0.50 (116)
	06_96	0.41 (46)	--
	combined	0.53 (543)	0.47 (249)
IM767	02_17	0.45 (53)	0.56 (122)
	02_48	0.54 (79)	0.49 (84)
	02_68	0.56 (39)	0.49 (141)
	06_39	0.55 (107)	--
	combined	0.53 (278)	0.51 (347)
SF	08_60	0.77 (104)****	0.73 (75)***
	12_09	0.50 (111)	0.54 (41)
	combined	0.62 (215)**	0.66 (116)*

[1]Individual IDs for F_2 progeny from $BG_4$275-IM767 crosses. At *hms1*, all F_2 individuals used were heterozygous for IM62 and IM767 alleles; at *hms2*, individuals used were homozygous for IM62, IM767, or SF alleles (see text for details).

[2]Percent IM62 alleles at *hms1* transmitted to progeny from IM62-IM767 heterozygous parent. Value given in parentheses is the number of progeny assessed.

* $P < 0.05$, ** $P < 0.01$, *** $P < 0.005$, **** $P < 0.0001$ based on X^2 tests of observed genotype frequencies versus the Mendelian expectation.

Figure 1

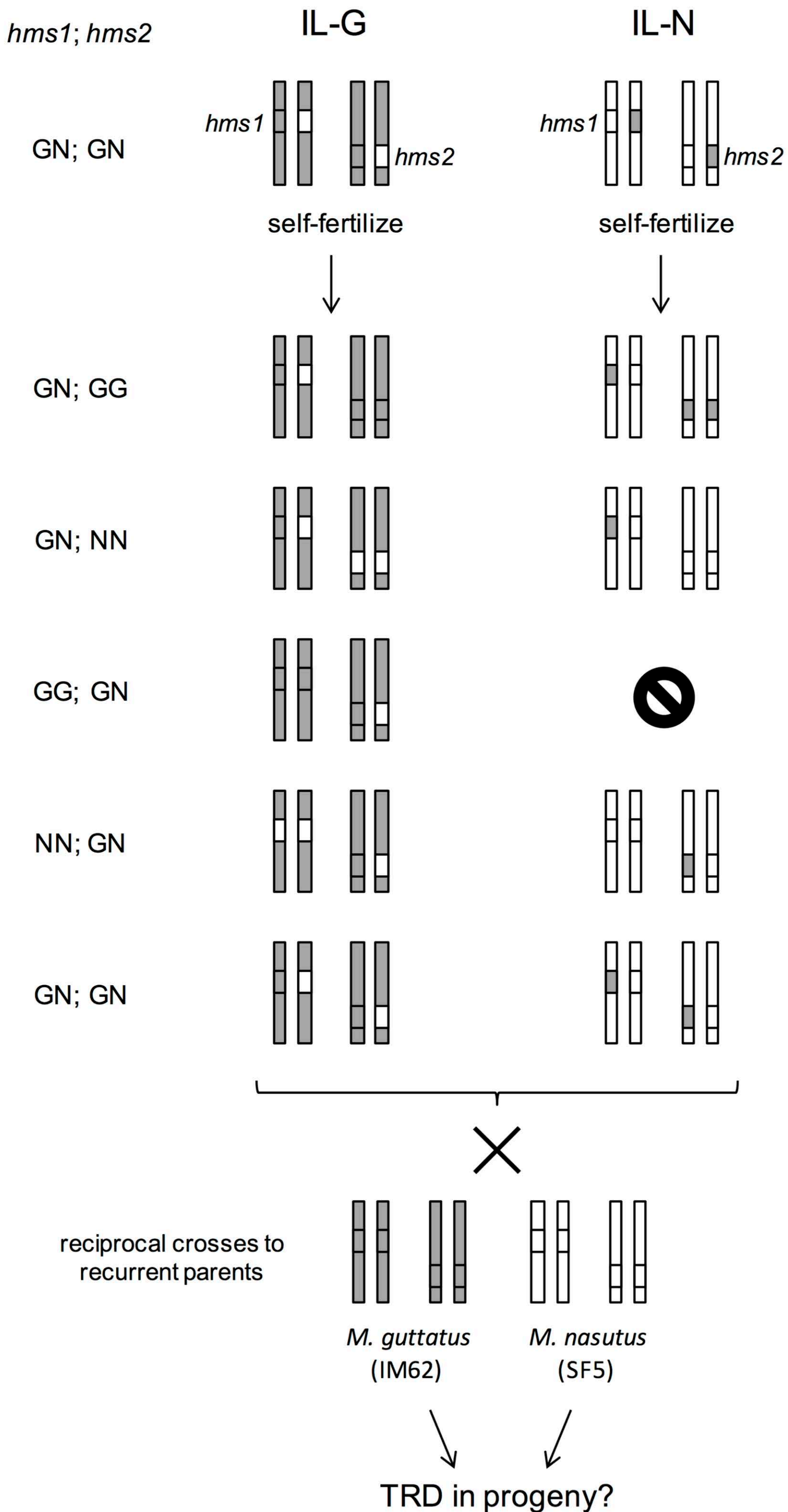

Figure 1. Crossing design for backcross experiment using introgression lines (ILs). For each genotype, two chromosome pairs are shown (one with *hms1* and one with *hms2*). We constructed two sets of ILs with heterozygous introgressions at both *hms1* and *hms2*; the IL-G has an *M. guttatus* genetic background (grey shading) and the IL-N has an *M. nasutus* genetic background (white). These doubly heterozygous ILs were self-fertilized to generate progeny with two-locus genotypes that are heterozygous at *hms1* and/or *hms2*. These five progeny types were then reciprocally backcrossed to *M. guttatus* and *M. nasutus*. G = *M. guttatus* allele (grey) ; N = *M. nasutus* allele (white).

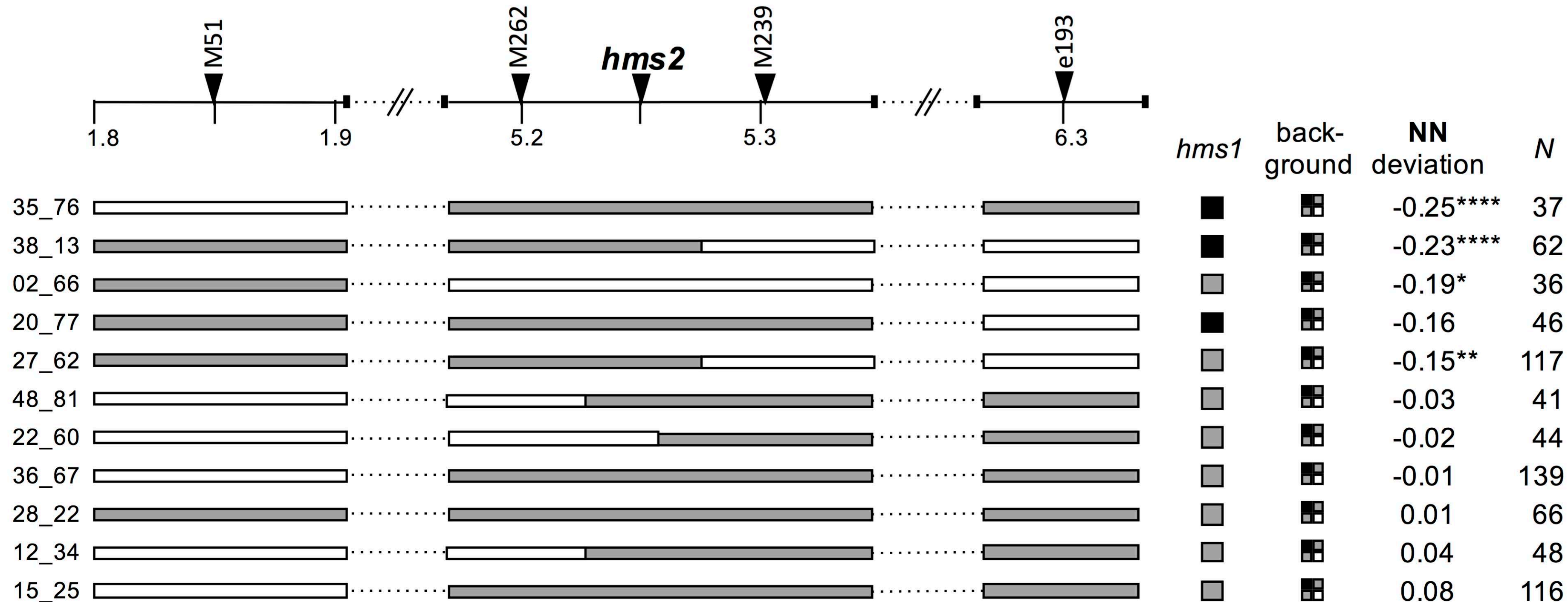

Figure 2. Genetic dissection of *hms2*-linked TRD in *Mimulus*. A physical map of ~4.5 Mb the *hms2* region is shown, including the positions of genetic markers (indicated with triangles along the top). F_2 recombinants are shown with horizontal bars representing genotypes in the genomic region linked to *hms2* and squares indicating genotypes at *hms1* and across the genetic background (white = *M. nasutus* homozygote, grey = heterozygote, black = *M. guttatus* homozygote). Deviation from the Mendelian expectation (0.25) of *M. nasutus* homozygotes (NN) in the F_3 progeny is given. *N* indicates the number of F_3 progeny scored from each individual. * $P < 0.05$, ** $P < 0.01$, *** $P < 0.005$, **** $P < 0.0001$ based on X^2 tests of observed frequencies versus the Mendelian expectation.

Figure 3

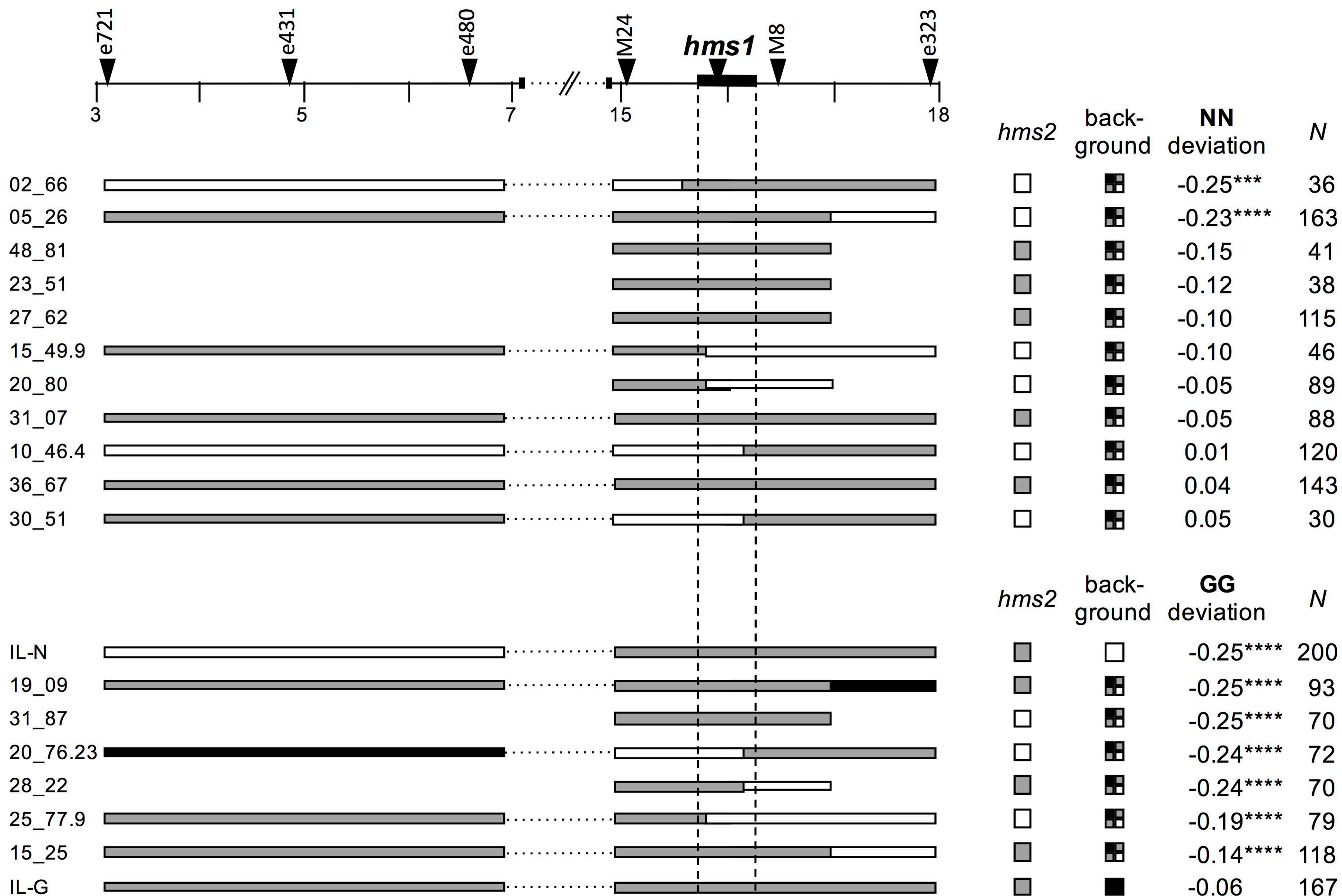

Figure 3. Genetic dissection of *hms1*-linked TRD in *Mimulus*. A physical map of 15 Mb the *hms1* region is shown, including the positions of genetic markers (indicated with triangles along the top) and the 320-kb *hms1* haplotype (shown as a solid black bar with dotted lines extending downwards). F_2 recombinants are shown with horizontal bars representing genotypes in the genomic region linked to *hms1* and squares indicating genotypes at *hms2* and across the genetic background (white = *M. nasutus* homozygote, grey = heterozygote, black = *M. guttatus* homozygote). Deviation from the Mendelian expectation (0.25) of *M. nasutus* homozygotes (NN) in the F_3 progeny is given for the top group of 11 F_2 recombinants. Deviation from the Mendelian expectation (0.25) of *M. guttatus* homozygotes (GG) in the F_3 progeny is given for the bottom group of six F_2 recombinants and the doubly heterozygous ILs. *N* indicates the number of F_3 progeny scored from each individual. *** $P < 0.005$, **** $P < 0.0001$ based on X^2 tests of observed frequencies versus the Mendelian expectation.

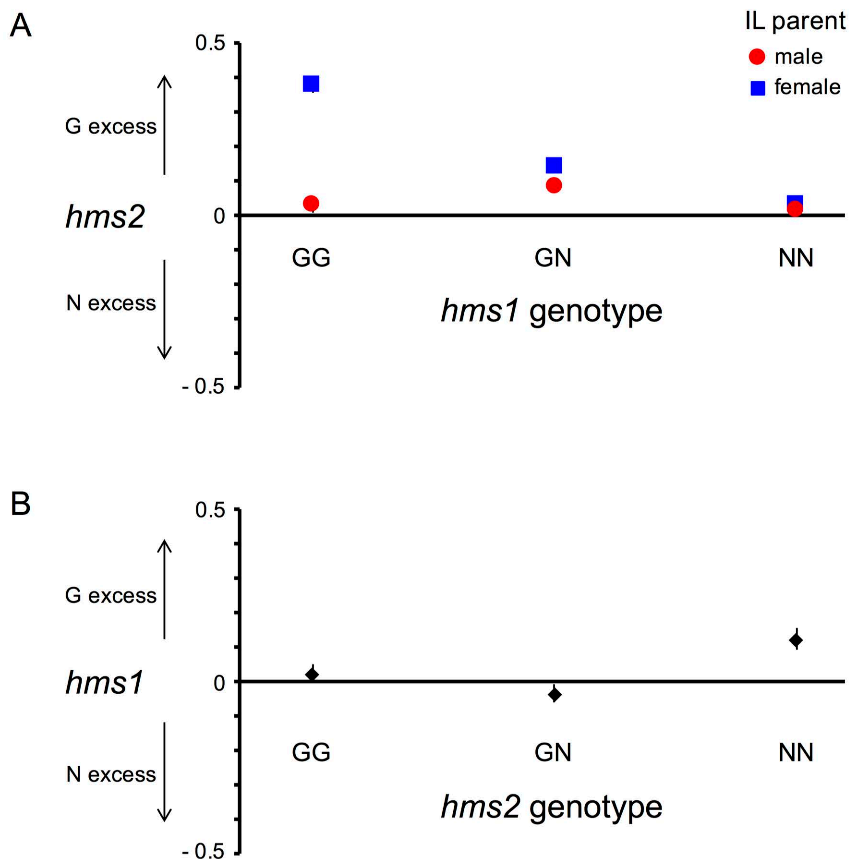

Figure S1. Transmission ratio distortion at *hms1* and *hms2* in IL-backcross progeny. The vertical position of each symbol shows the magnitude and direction of the deviation of allelic transmission from the Mendelian expectation (0.5). *M. guttatus* deviations are graphed directly [deviation = *f*(N – 0.5)], and the *M. nasutus* deviations are graphed as negative [deviation = - (*f*(N-0.25)]. Thus, values above zero indicate excess of *M. guttatus* alleles and values below zero indicate excess of *M. nasutus* alleles. G = *M. guttatus* allele, N = *M. nasutus* allele. A) Allelic transmission of *hms2* in the progeny of IL-backcrosses is significantly affected by IL parental genotype at *hms1* ($F = 37.6919$, $P < 0.0001$), cross direction ($F = 72.3339$, $P < 0.0001$), and their interaction ($F = 31.8353$, $P < 0.0001$). B) Allelic transmission of *hms1* in the progeny of IL-backcrosses is significantly affected by IL parental genotype at *hms1* ($F = 7.7977$, $P = 0.0043$).

Figure S2

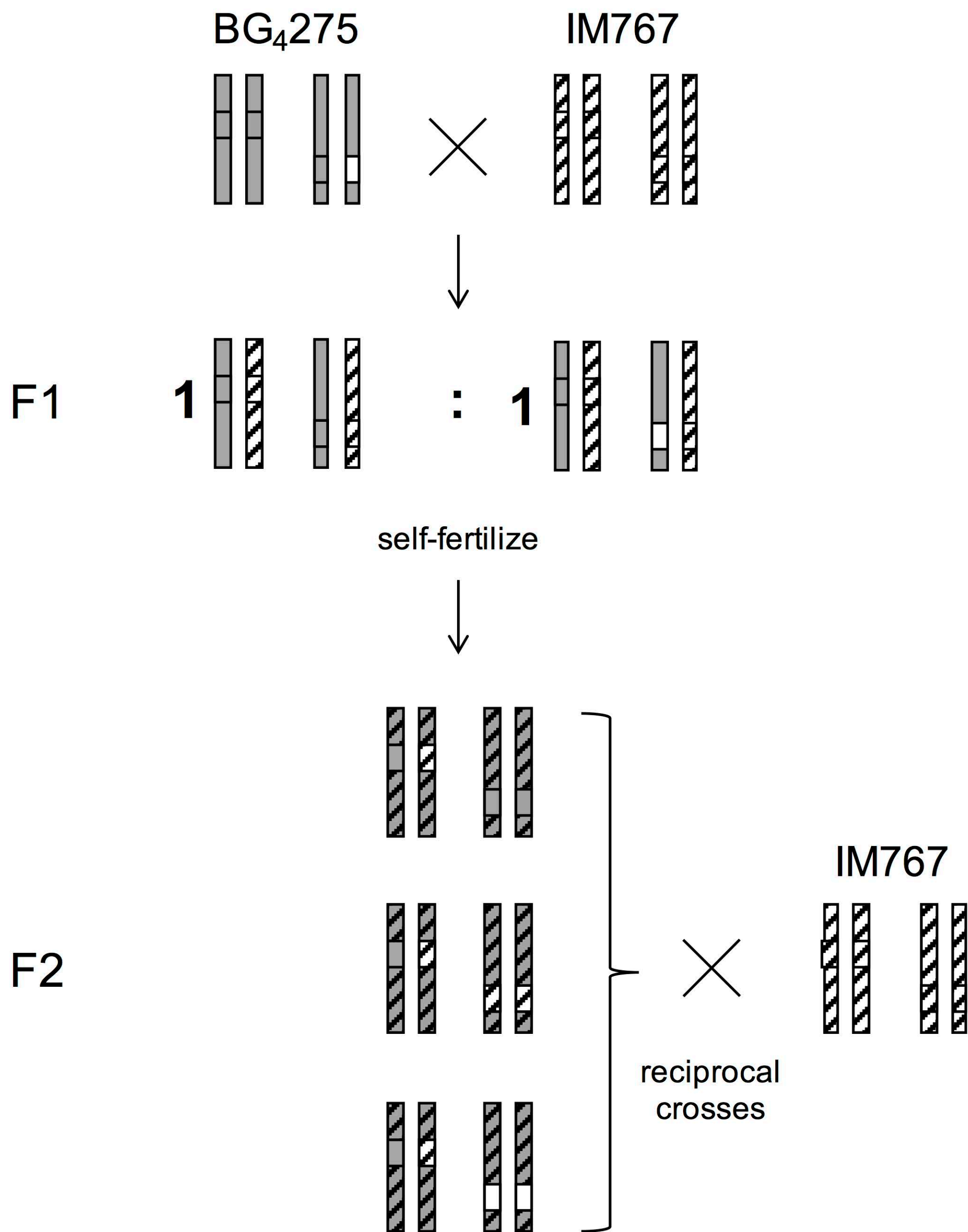

Figure S2. Crossing scheme for investigating the effect of *M. nasutus* (SF5) homozygosity at *hms2* on within-*M. guttatus* TRD at *hms1*. For each genotype, two chromosome pairs are shown (one with *hms1* and one with *hms2*). We intercrossed IM767 (stripes) and BG_4.275, which carries a heterozygous SF5 introgression (white) at *hms2* against an IM62 (grey shading) genetic background. The resulting progeny segregate 1:1 for two different genotypes at *hms2*: IM62-IM767 heterozygotes and SF5-IM767 heterozygotes (the remaining genetic background is heterozygous for IM62 and IM767 alleles). We genotyped F_2 progeny with *hms*-linked markers to identify IM62-IM767 *hms1* heterozygotes in combination with three different *hms2* genotypes: IM62 homozygotes, IM767 homozygotes, and SF5 homozygotes. Individuals with each of these three two-locus genotypes were then reciprocally backcrossed to IM767 to assess TRD at *hms1*. Note that the genetic background of the F_2 progeny are expected to segregate 1:2:1 for IM62 homozygotes, heterozygotes, and IM767 homozygotes (grey shading with stripes).

Table S1. Observed and expected genotype frequencies at *hms1* and *hms2* in F_2 hybrids (N = 5487).

genotype *hms1*; *hms2*	O	E: Mendelian	E: GN inviable, 1 parent[1]	E: GN inviable, 2 parents[2]	E: GN partial inviablity, 1 parent[3]
GG; GG	0.099	0.0625	0.083	0.109	0.076
GG; GN	0.100	0.1250	0.083	0	0.098
GG; NN	0.022	0.0625	0	0	0.022
GN; GG	0.208	0.1250	0.165	0.218	0.152
GN; GN	0.268	0.2500	0.248	0.218	0.25
GN; NN	0.071	0.1250	0.083	0	0.098
NN; GG	0.070	0.0625	0.083	0.109	0.076
NN; GN	0.117	0.1250	0.165	0.218	0.152
NN; NN	0.047	0.0625	0.083	0.109	0.076

[1] Expected F_2 genotype frequencies if 100% of $hms1_G$; $hms2_N$ gametes are inviable in one parent. Observed F_2 genotype counts significantly differ from this expectation (X^2 = 325.725, d.f. = 8, P <0.0001). G = *M. guttatus* allele, N = *M. nasutus* allele.
[2] Expected F_2 genotype frequencies if 100% of $hms1_G$; $hms2_N$ gametes are inviable in both parents. Observed F_2 genotype counts significantly differ from this expectation (X^2 = 1853.55, d.f. = 8, P <0.0001).
[3] Expected F_2 genotype frequencies if 65% of $hms1_G$; $hms2_N$ gametes are inviable in one parent. This threshold of inviability was set by assuming the observed $hms1_{GG}$; $hms2_{NN}$ F_2 genotype frequency was determined solely by partial inviability through one parent. Observed F_2 genotype counts significantly differ from this expectation (X^2 = 156.892, d.f. = 8, P <0.0001).

bioRxiv preprint doi: https://doi.org/10.1101/150854; this version posted June 16, 2017. The copyright holder for this preprint (which was not certified by peer review) is the author/funder, who has granted bioRxiv a license to display the preprint in perpetuity. It is made available under aCC-BY-ND 4.0 International license.

Table S2. The severity of under-transmission of $hms1_G$; $hms2_N$ gametes (measured as the deviation from the Mendelian expectation of 0.25) in IL-backcrosses is affected by genetic background, cross direction, and identity of the recurrent parent.

Effect[1]	df	*F*	*P*	LSM	
Background[2]	1	8.259	0.045	G: -0.095	N: -0.149
Cross direction[3]	1	30.910	0.005	♂: -0.174	♀: -0.070
Recurrent parent[4]	1	7.359	0.053	G: -0.147	N: -0.097

[1]Effects assessed by ANOVA with degrees of freedom (df), F-ratio (*F*), p-values (*P*), and least squares means (LSM) indicated.
[2]Crosses performed using fourth-generation NILs. *M. nasutus* background = BN_4; *M. guttatus* background = BG_4.
[3]Cross direction indicates whether the NIL was used as the paternal (♂) or maternal (♀) parent.
[4]Testcrosses were to the IM62 line of *M. guttatus* (G) or the SF line of *M. nasutus* (N).

bioRxiv preprint doi: https://doi.org/10.1101/150854; this version posted June 16, 2017. The copyright holder for this preprint (which was not certified by peer review) is the author/funder, who has granted bioRxiv a license to display the preprint in perpetuity. It is made available under aCC-BY-ND 4.0 International license.

Table S3. Genotype counts for progeny from reciprocal backcrosses between IM62 and the doubly heterozygous IL-N ($hms1_{GN}$; $hms2_{GN}$).

	hms1; *hms2* genotype			
Maternal parent	GG; GG	GG; GN	GN; GG	GN; GN
IL-N	105	45	105	99
IM62	35	3	31	35